The restricted three-body problem and convexity

Otto van Koert (joint with Bowen Liu)

Introduction: some history

In the first book of "Philosophiæ Naturalis Principia Mathematica" (1687), Newton solved the Kepler (two-body) problem, and described the three-body problem, which he could not solve.

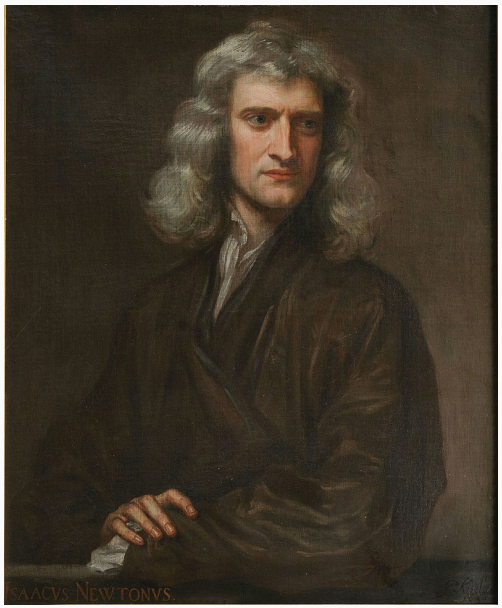

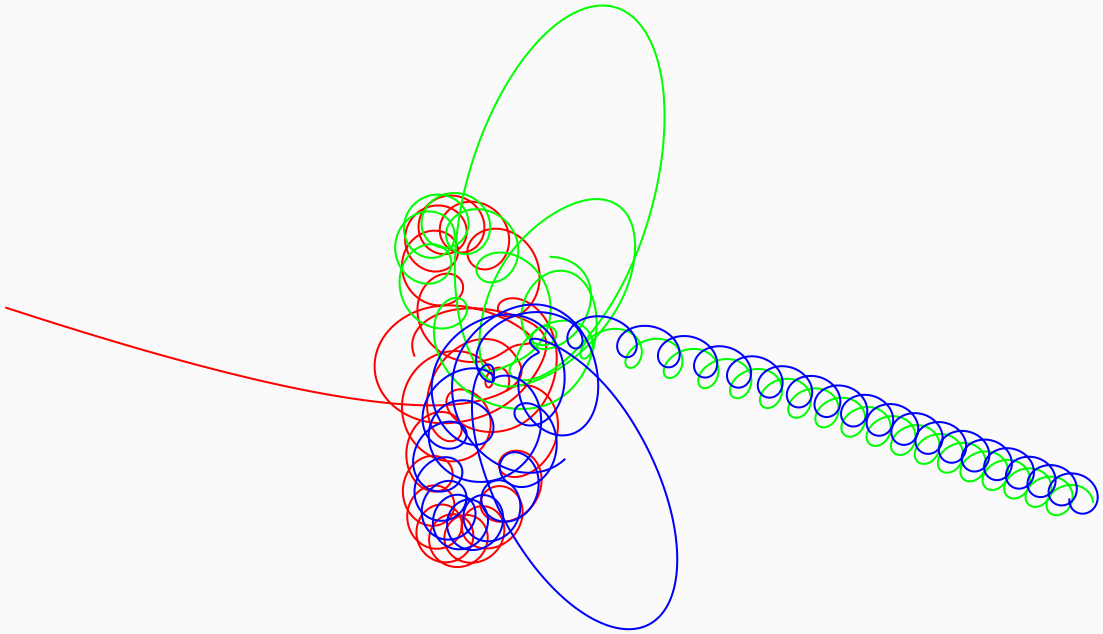

Figure 1: Newton (taken from wikipedia) and the three-body problem

Let us describe the N-body problem (see video of Scott Manley). Fix constants $m_1, \ldots, m_N > 0$. The N-body problem is to understand solutions to the differential equation (usually initial value problem) for $(q_1, \ldots, q_N, v_1, \ldots, v_N) \in \mathbb{R}^{3N} \times \mathbb{R}^{3N}$,

$$\begin{aligned} \frac{dq_i}{dt} &= v_i \\ m_i \frac{dv_i}{dt} &= \sum_{j \neq i} \frac{m_i m_j (q_j - q_i)}{\|q_j - q_i\|^3}. \end{aligned}$$

We focus on the three-body problem ($N = 3$) because

- it is the easiest after the two-body problem
- it is not integrable (shown by Poincaré)
- it was the first problem for which this and the presence of chaos was shown.

Poincaré and RTBP

- on the occasion of the 60th birthday of king Oscar of Sweden in 1889, there was a prize contest for "solving the three-body problem"
- the referees for the contest were Mittag-Leffler and Weierstrass

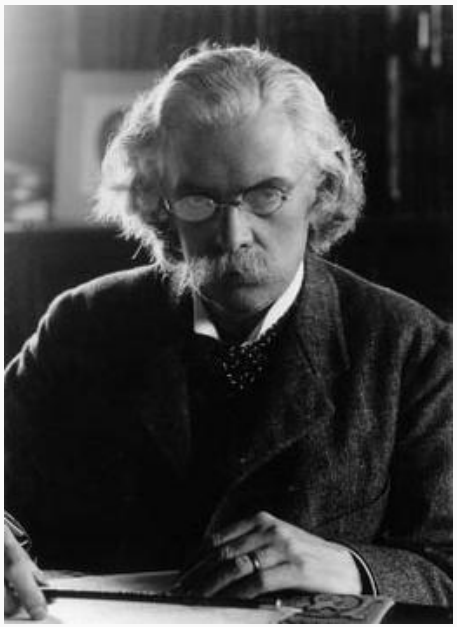

Figure 2: Mittag-Leffler, Poincaré and Weierstrass (taken from wikipedia)

- despite not actually solving the problem, Poincaré was awarded the prize. In the final paragraph of his report, Weierstrass did indicate that he found the paper difficult to read, and complained about the lack of complete rigor.
- In his paper, Poincaré "proved" the stability of the solar system
- Poincaré found a mistake and informed Mittag-Leffler. In order to not embarass the king, he payed for the recall of all printed copies of his paper (more than the prize money). The revised version outlines in a single paragraph the Smale horseshoe about 60-70 years before Smale, indicating potential chaos.

In his several books on this topic, Poincaré developed many useful ideas in topology and dynamics: one of them is the notion of a surface of section.

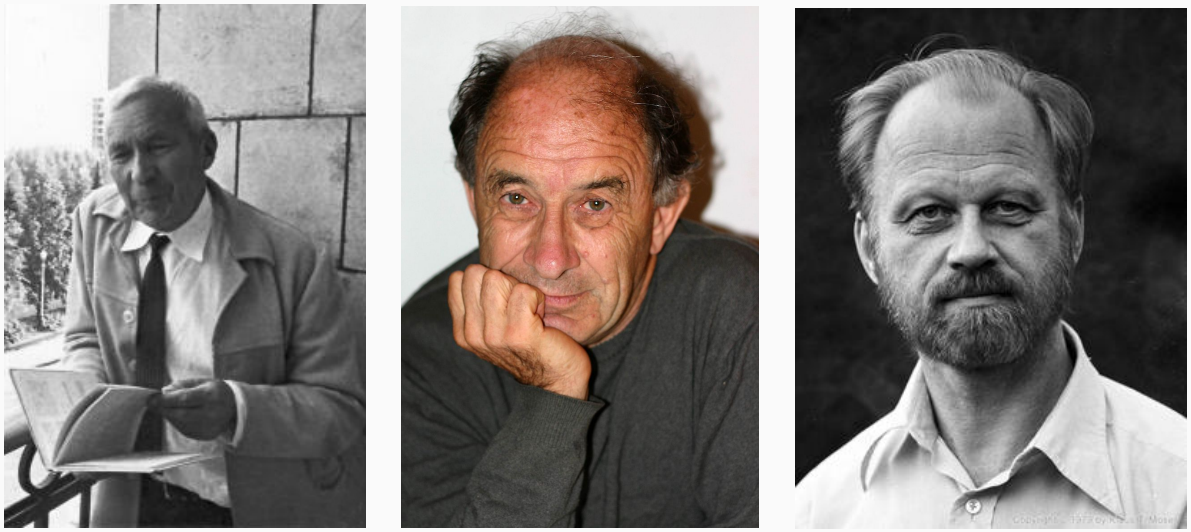

Figure 3: Kolmogorov, Arnold and Moser (taken from wikipedia) all contributed to what is now known as KAM theory

The stability story does not end here; Arnold proved a version of the so-called KAM theorem which he applied to the solar system.

- in his application the non-degeneracy condition of the Hamiltonian is not satisfied: this was fixed by Chierchia and Pinzari in 2011

- more seriously, KAM theorem depends on a kind of implicit function theorem, and the perturbation needs to be sufficiently small.
- Numerical work (notably by Laskar) strongly suggests that the solar system does not satisfy this condition and is not as stable as initially believed.

Let us return to 1910 and Poincaré's ideas.

His results lead Poincaré to conjecture the following in 1912.

Theorem (Poincaré's last geometric theorem, proved by Birkhoff in 1913)
Every area-preserving, orientation-preserving homeomorphism of an annulus that rotates the two boundaries in opposite directions (this is known as a twist map) has at least two fixed points.

The goal was to apply this to RTBP by finding a GSS and checking the twist condition.

This theorem was not provable with algebraic topology techniques: it has some essential symplectic nature. It lead Arnold to conjecture the well-known "Arnold conjectures". Today, we focus on the construction of GSS's.

Global hypersurfaces of section

A global surface of section is a tool to convert the dynamics of flows to the dynamics of maps: we consider a compact, oriented smooth manifold with non-singular flow ϕ_t.

Definition
Call an oriented, compact hypersurface Σ in Y a *global hypersurface of section* for ϕ_t if

- the set $\partial\Sigma$ is an invariant set for the flow ϕ_t (if non-empty);
- the flow ϕ_t is positively transverse to the interior of Σ;
- for all $x \in Y \setminus \partial\Sigma$ there are $t_+ > 0$ and $t_- < 0$ such that $\phi_{t_+}(x) \in \Sigma$ and $\phi_{t_-}(x) \in \Sigma$.

Remark

The main point is that this can be used to discretize the global dynamics.

A restriction for the higher-dimensional case is that invariant sets of dimension greater than 1 tend to be unstable... (KAM doesn't apply to the invariant sets needed here)

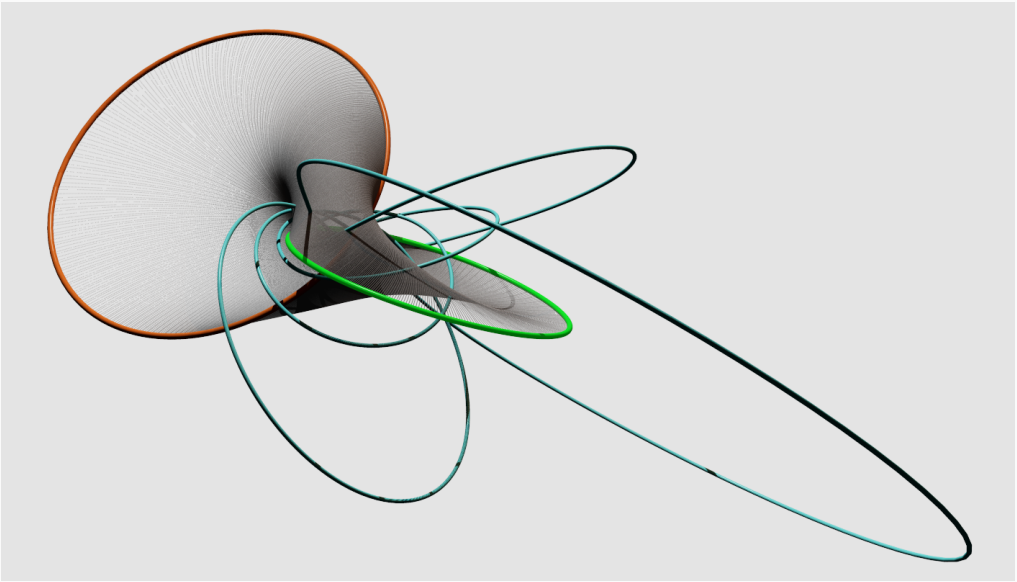

Figure 4: A global surface of section (after stereographic projection) and some periodic orbits

Examples and non-examples

- suppose that $P \to \Sigma_g$ is a a prequantization bundle with Euler number e; then there is a GSS diffeomorphic to Σ_g minus e open disks for the (periodic) Reeb flow; the return map is the identity.
- geodesic flow on hyperbolic surface: this is a Reeb flow on $ST^*\Sigma_g$. There is a GSS diffeomorphic to a torus minus a couple of open disks (depends on genus); the return map can be computed explicitly
- the horocycle flow $ST^*\Sigma_g$ admits no GSS.

Remark
A contact manifold (Y, α) is the level set of an autonomous Hamiltonian H on a symplectic manifold (M, ω) with the property that there is a vector field X that is transverse to this level set with $\mathcal{L}_X \omega = \omega$. A certain reparametrization of the Hamilonian flow on this level set is then called Reeb flow.

The existence and construction of the GSS's is hence of interest.

Definition
A contact 3-manifold is dynamically convex if the Conley-Zehnder index (more on that later) $\mu_{CZ}(\gamma) \geq 3$ for every contractible periodic Reeb orbit γ.

Theorem (see Hofer-Wysocki-Zehnder, but also many others)
Compact, strictly convex hypersurfaces in $\mathbb{R}^4$ are dynamically convex.

Theorem (HWZ 1998)
If $Y = H^{-1}(c)$ is dynamically convex, then Y admits a disk-like GSS.

A strong point in this theorem is that this gives a GSS with the simplest possible topology. The construction is also relatively explicit and no further genericity conditions are needed.

Hryniewicz, Salomão (later also with Wysocki) added several improvements allowing the construction of GSS's with more general genus-0 surfaces.

However, the following is now also known:

Theorem (Contreras-Mazzucchelli, Colin-Dehornoy-Hryniewicz-Rechtman)
Generically, the Reeb flow on a compact contact 3-manifold admits a global surface of section.

In this case, there is no control on the topology of the GSS, and one can show that the topology of the GSS can become arbitrarily complicated.

Index and convexity

Given a Hamiltonian orbit $x_t = Fl_t^{X_H}(x_0)$ in a symplectic manifold (W, ω) and a trivialization ϵ of $(TW, \omega = d\lambda)$ along x_t, we define the **Robbin-Salamon index** of x_t as

$$\mu_{RS}(x_t, \epsilon) := \mu_{RS}(\epsilon_t^{-1} \circ dFl_t^{X_{H_t}} \circ \epsilon_0).$$

Here the **Robbin-Salamon index** of symplectic path ψ is the "intersection number" of ψ with the Maslov cycle

$$V = \{A \in Sp(2n) \mid \det(A - id) = 0\}$$

Remark

In case the endpoint of the path x_t is non-degenerate, i.e. the linear map $\epsilon_{t_e}^{-1} \circ dFl_{t_e}^{X_{H_t}} \circ \epsilon_0 - id$ is invertible, then this index is also called Conley-Zehnder index.

Figure 5: Part of the Maslov cycle in $Sp(2) \cong S^1 \times \mathbb{R}^2$ lifted to a fundamental domain in $\mathbb{R}^3$

Definition
We call (Y^3, α) **dynamically convex** if all contractible periodic Reeb orbits have Conley-Zehnder index at least 3.

Toy example with holomorphic curves

Consider the Hamiltonian on $\mathbb{C}^2 - \{0\} \cong \mathbb{R} \times S^3$ for the Hopf fibration

$$H(z, w) = |z|^2 + |w|^2.$$

Consider the foliation by holomorphic planes $z \mapsto (z, a)$. These are all asymptotic to the Hopf fiber $(e^{i\phi}, 0)$. In the energy surface we get the global surfaces of section

$$z \mapsto \left(\frac{z}{\sqrt{|z|^2 + |a|^2}}, \frac{a}{\sqrt{|z|^2 + |a|^2}}\right).$$

Remark

Of course, the dynamics here are trivial making it obvious that this disk is a global surface of section.

Moduli space

In the above example, the standard complex structure maps the radially outward pointing field to the Reeb vector field. It also sends the contact planes ξ to ξ, and is "scale"-invariant

Definition
We call this an SFT-like almost complex structure. Write J.

Consider $u : \mathbb{C} \to \mathbb{R} \times S^3$ satisfying the equation

$$J \circ du = du \circ i, \lim_{r \to \infty} u(r, \phi) = \{\infty\} \times \gamma(\phi)$$

We collect solutions to this equation (mod reparametrization) in the moduli space $\mathcal{M}(\gamma)$.

Compact moduli space

In the toy example (with complex coordinates)

$$\mathcal{M}(\gamma) = \{[u_a : z \mapsto (z, a)]\}$$

This space has an $\mathbb{R}$ action (moving the plane up and down), and here $\mathcal{M}(\gamma)/\mathbb{R} \cong S^1$ is compact.

From the equation we also see that if u is immersed, then the Reeb field is transverse to $\pi_{S^3} \circ u$. We conclude that each $\pi_{S^3} \circ u_a$ is a global surface of section.

Remark
The proof of HWZ's theorem is more complicated, but the above cartoon sketches some of the ideas.

Systems of interest

Definition
A **Stark-Zeeman system** models the dynamics of an electron attracted by a proton in the presence of a magnetic field.

We use a twisted symplectic form

$$\omega = dp \wedge dq + \pi^* \sigma_B,$$

with $\sigma_B = \frac{1}{2} \sum B_{ij} dq_i \wedge dq_j$. The Hamiltonian is given by

$$H = \frac{1}{2} \|p\|^2 + V_0(q) + V_1(q),$$

where $V_0(q) = -\frac{1}{\|q\|}$, and V_1 is a smooth potential.

Remark
We will assume that the magnetic field is exact with primitive 1-form A. Then with respect to $dp \wedge dq$ we can write

$$H = \frac{1}{2}\|p + A\|^2 + V_0(q) + V_q(q).$$

These systems include

- Systems from celestial mechanics: RTBP, Hill's lunar
- Diamagnetic Kepler problem

Why?

- These systems share many technical features (such as regularization), and are of interest in physics.

Diamagnetic Kepler problem

We consider an electron in $\mathbb{R}^3$ in a constant magnetic field, attracted by a proton at $q = 0$.

The Hamiltonian describing its dynamics is in cylindrical coordinates given by

$$H = \frac{1}{2}\left(p_\rho^2 + p_z^2 + \frac{p_\theta^2}{\rho^2} - Bp_\theta\right) + \frac{B^2}{8}\rho^2 - \frac{1}{\sqrt{\rho^2 + z^2}}$$

For the diamagnetic Kepler problem we consider the case when the angular momentum $p_\theta = 0$.

Remark
This system is of interest because of its surprisingly complicated dynamics.

Some periodic orbits in the diamagnetic Kepler problem,

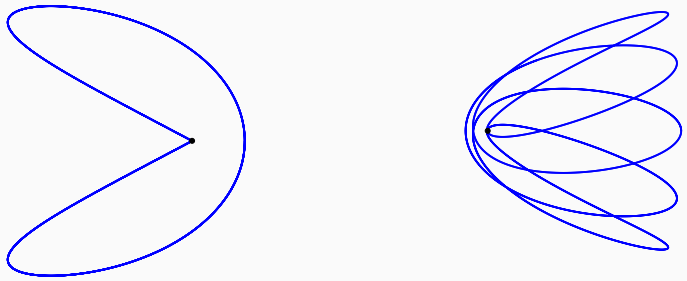

Proposition
Level sets $H = -c$ of diamagnetic Kepler problem is convex for

$$c > \frac{(-300 + 156\sqrt{(5)})^{1/3}}{4} \sim 0.9$$

.

Remark
With some numerical work, one can prove that dynamical convexity will fail for much smaller c: the simple bounce orbits start as elliptic orbits in $\mathbb{R}P^3$ with index 1, but as c becomes smaller, the trace of the return map becomes negative, so the index of the double cover drops.

Review of PRTBP

We consider a "massless" particle affected by by particles at $q_i(t)$ for $i = 1, 2$.

$$H(q,p) = \frac{1}{2}\|p\|^2 - \sum_{i=1}^{2} \frac{m_i}{\|q - q_i(t)\|}$$

Suppose now q_1 and q_2 move around each other in circular orbits. It was discovered by Jacobi that then the problem turns out to admit an integral after going to a rotating frame.

This is the **planar, restricted three-body problem** (PRTBP).

The **Jacobi Hamiltonian** is the autonomous Hamiltonian

$$H(q,p) = \frac{1}{2}\|p\|^2 + p^t J_0 q - \frac{1-\mu}{\|q+\mu\|} - \frac{\mu}{\|q-1+\mu\|}$$

Lagrange points

H_{RTBP} has five critical points, known as Lagrange points L_1, L_2, L_3 (all index 1) and L_4, L_5 (index 2).

For $E < H(L_1)$, levels sets of H have three components, which in the Hill's region to the sets bounded by the red curves.

Remark
A component of the energy surface is diffeomorphic to $S^1 \times \mathbb{R}^2$: it can be compactified to $\mathbb{R}P^3$ by attaching a circle.

Hill's region (level sets of the effective potential)

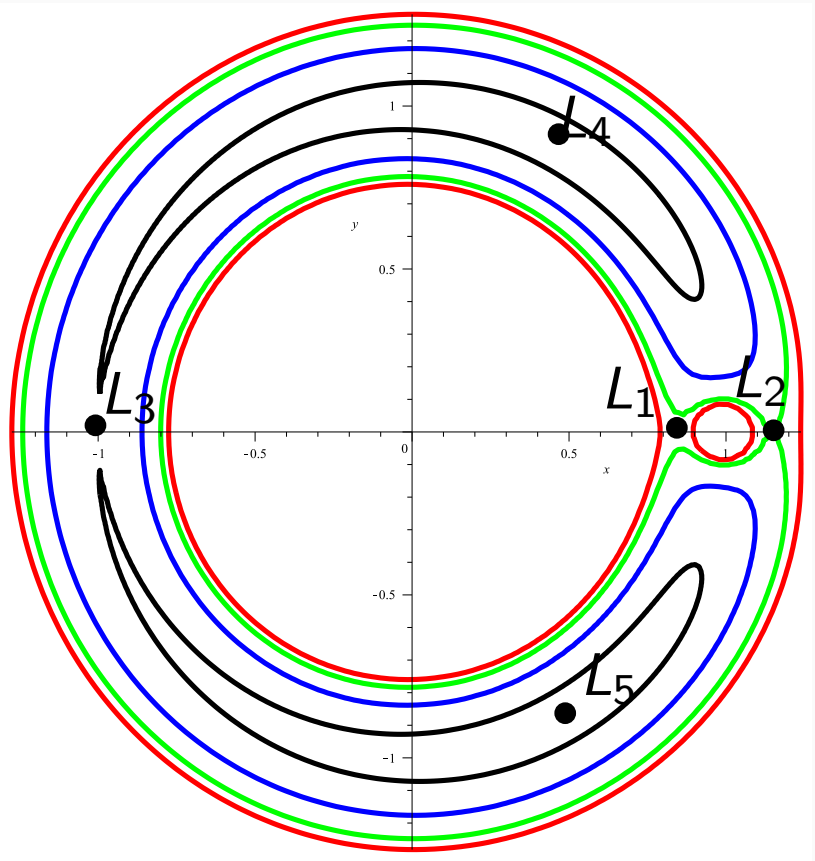

Levi-Civita regularization

This $\mathbb{R}P^3$ is covered by S^3. The Levi-Civita transformation, which is symplectic up to a factor 4, performs these two steps:

$$q = 2z^2$$
$$p = \frac{w}{\bar{z}}$$

For the Kepler Hamiltonian $(H = \frac{1}{2}|p|^2 - \frac{1}{|q|})$ we get

$$(H + c)|z|^2 = \frac{1}{2}(|w|^2 + 2c|z|^2) - 1.$$

Level set in RTBP

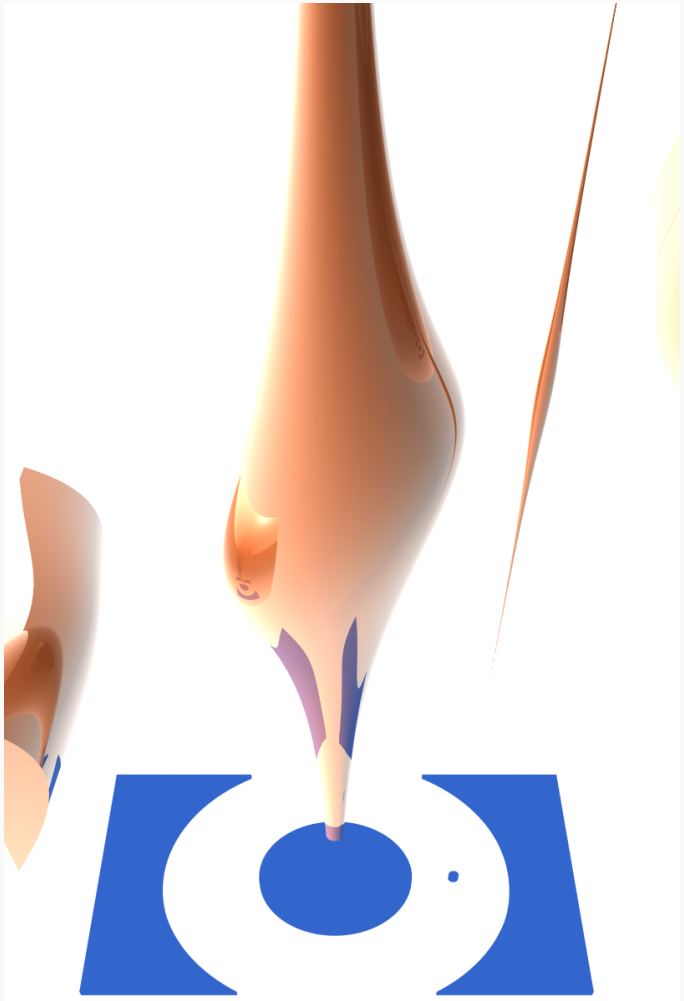

Theorem (Frauenfelder, vK, Zhao)
For $c > 3/2$, and for μ sufficiently small, RTBP is dynamically convex. Its Levi-Civita regularization is not convex. However, the composition of Ligon-Schaaf with Levi-Civita regularization is convex

The dynamical application is not new: it was already written explicitly in McGehee's thesis and goes back to Poincaré.

Theorem (Albers, Frauenfelder, Fish, Hofer, vK)
For $c > 3/2$, and for μ sufficiently large, RTBP is convex.

This gives global surfaces of section near the light primary.

Convexity below $H(L_1)$ and GSS's

Here is a schematic picture of convexity analytical results that are now known. With Bowen Liu, we investigated where convexity holds and where it doesn't hold.

Note that the Lyapunov orbit, born at L_1, has $\mu_{CZ} = 2$, so will break dynamical convexity for energies above $H(L_1)$.

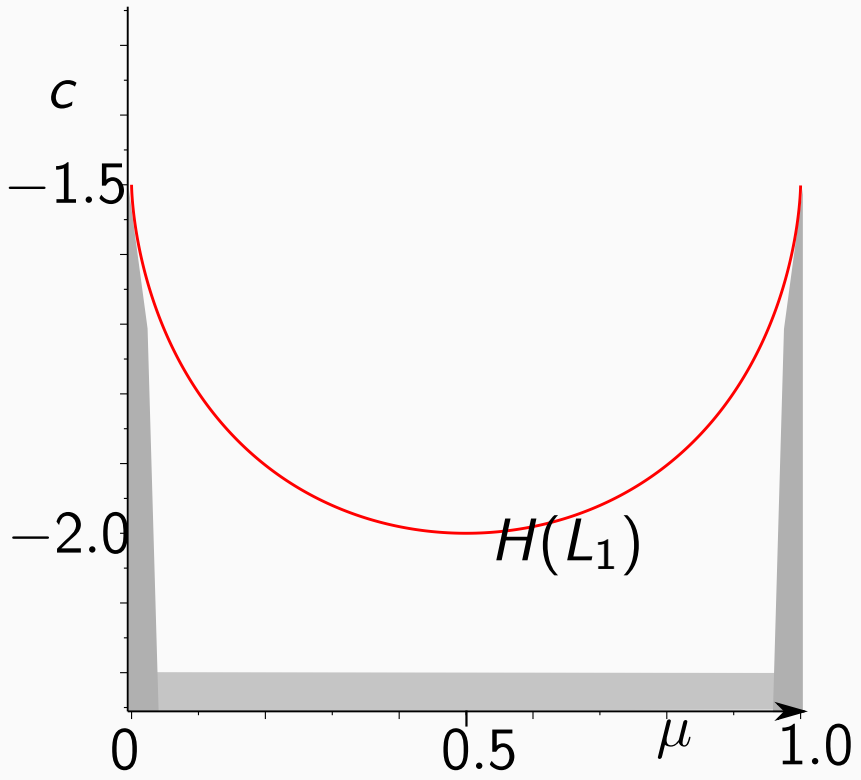

Theorem (Liu-vK)
There is no $\mu \in (0,1)$ such that both the component of the light primary and the heavy primary of the Levi-Civita regularization of the RTBP are convex.

The situation for other regularizations (eg. Birkhoff regularization) does not appear to be better. On the other hand, with interval arithmetic, we have also shown that

Theorem (Liu-vK)
For $\mu = 1/2$ and $c = 2.01$ ($c_{L_1} = 2$), the component $\Sigma^H_{1/2,2}$ is convex.

This leaves us with working directly with dynamical convexity.

Remark
Convexity is also useful to study the dynamics of the spatial RTBP.

Constructing GSS's

We now turn our attention to the actual construction of GSS's and an overview of the resulting return maps

- the HWZ construction can be put in a computer for numerical approximation.
- convexity can also be exploited in more ad hoc approaches.

The upshot is that we can numerically approximate the GSS's and look at the return map.

Return map for the disk (below L_1)

The return map for the disk
We obtain a return map by numerical integration.

- For small mass ratios or energies sufficiently far below the Lagrange point, the first return map behaves similar to the return map found by McGehee, $(r, \phi) \mapsto (r, \phi + f(r))$
- Strongly deformed for larger mass ratios ($\mu > 0.1$).

id

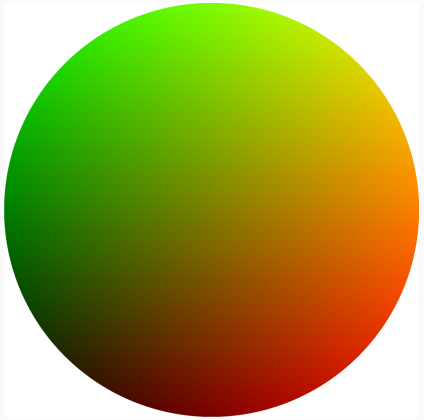

$\mu = 10^{-1}$, $c = 2$, τ

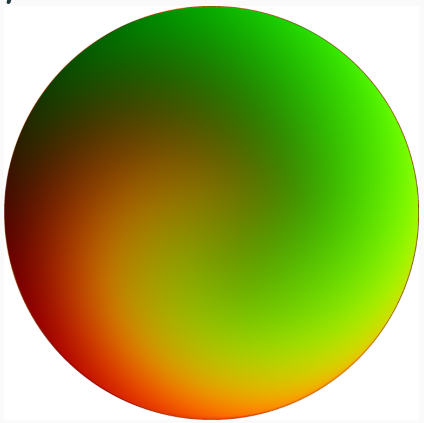

Behavior of iterates

We discretize the first return map τ and then compute iterates. (here $\mu = 0.1$, $c = 2$).

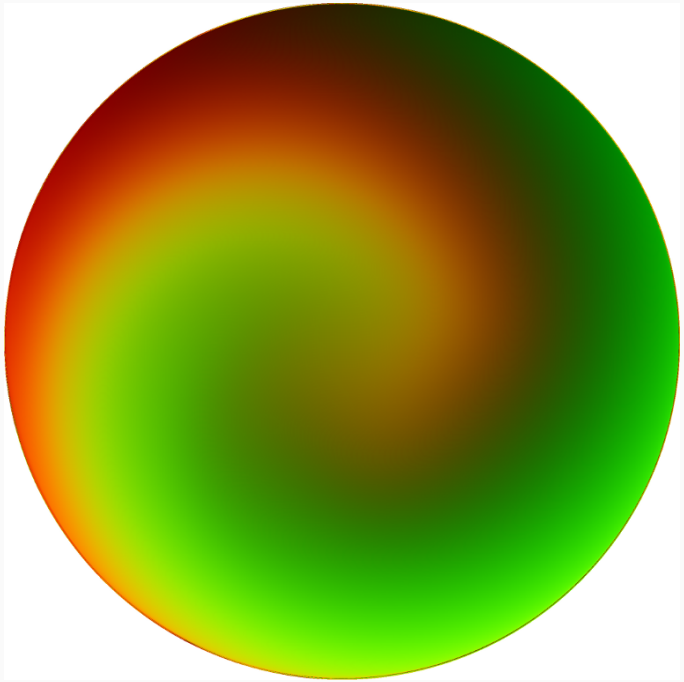

Figure 6: τ^2

Behavior of iterates

We discretize the first return map τ and then compute iterates. (here $\mu = 0.1$, $c = 2$).

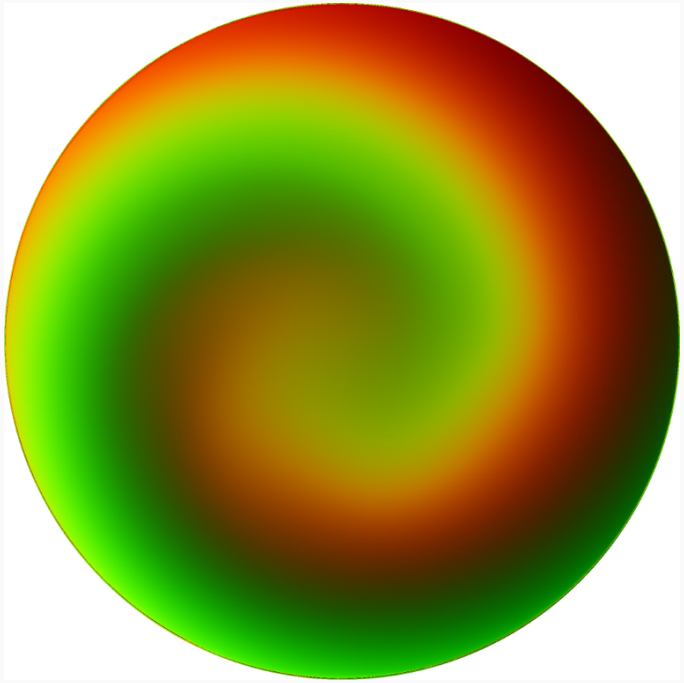

Figure 6: τ^3

Behavior of iterates

We discretize the first return map τ and then compute iterates. (here $\mu = 0.1$, $c = 2$).

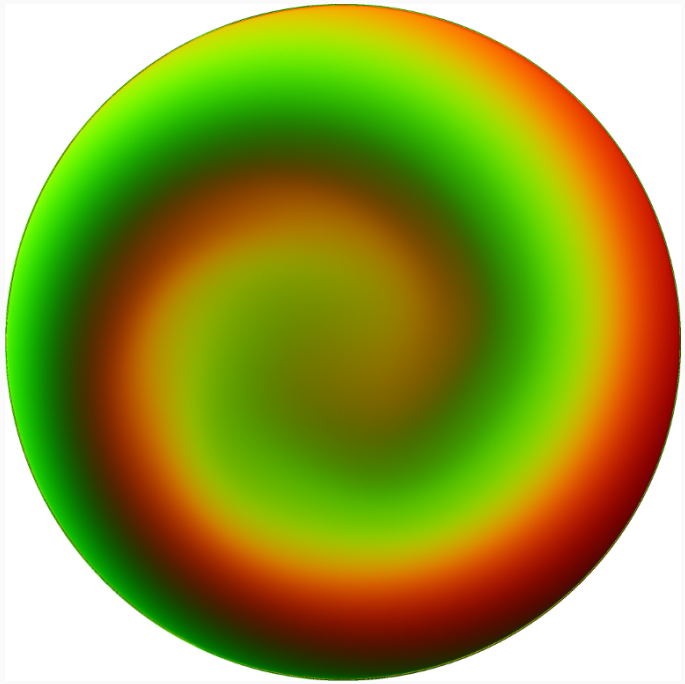

Figure 6: τ^4

Behavior of iterates

We discretize the first return map τ and then compute iterates. (here $\mu = 0.1$, $c = 2$).

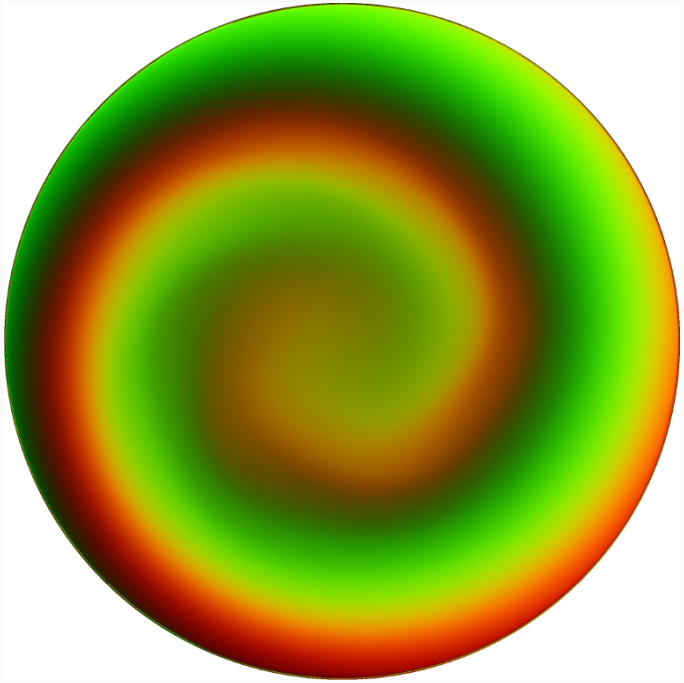

Figure 6: τ^5

Behavior of iterates

We discretize the first return map τ and then compute iterates. (here $\mu = 0.1$, $c = 2$).

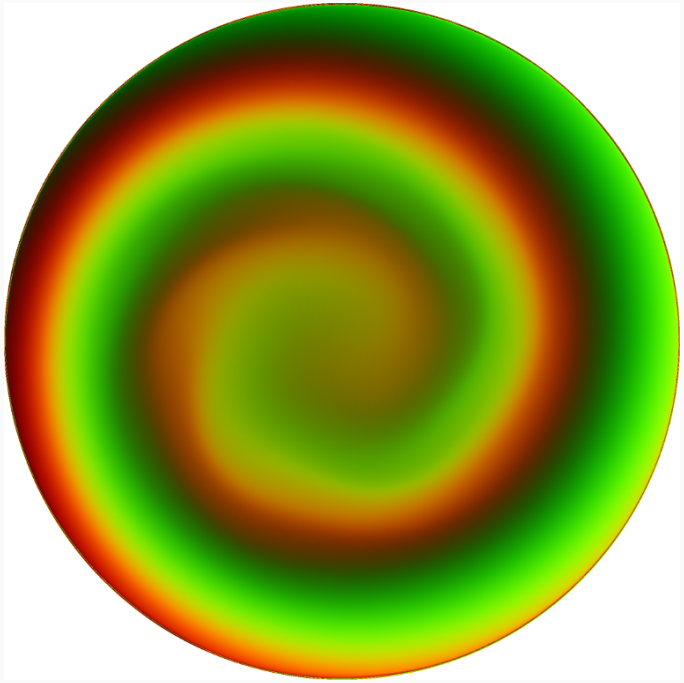

Figure 6: τ^6

Behavior of iterates

We discretize the first return map τ and then compute iterates. (here $\mu = 0.1$, $c = 2$).

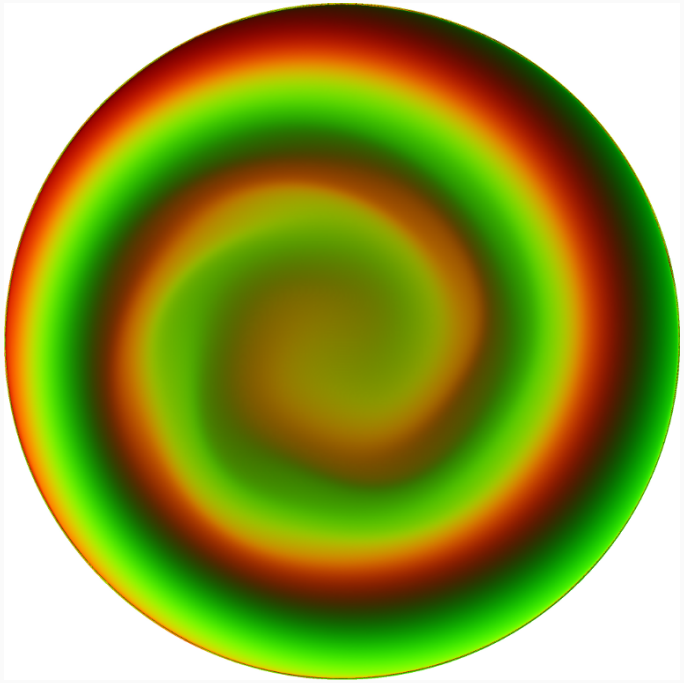

Figure 6: τ^7

Behavior of iterates

We discretize the first return map τ and then compute iterates. (here $\mu = 0.1$, $c = 2$).

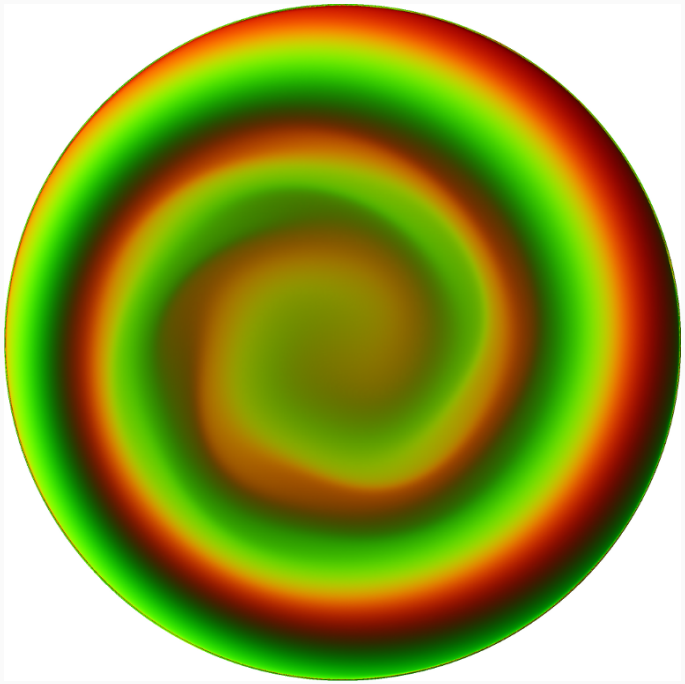

Figure 6: τ^8

Behavior of iterates

We discretize the first return map τ and then compute iterates. (here $\mu = 0.1$, $c = 2$).

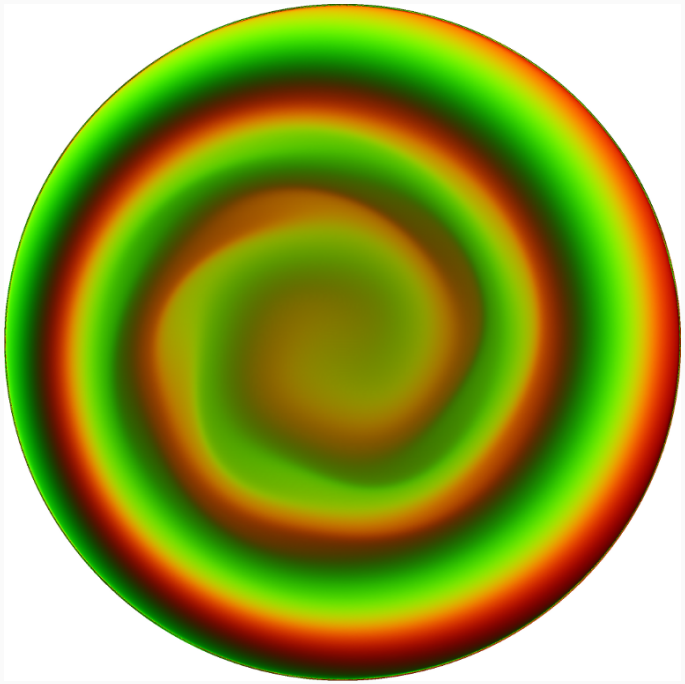

Figure 6: τ^9

Behavior of iterates

We discretize the first return map τ and then compute iterates. (here $\mu = 0.1$, $c = 2$).

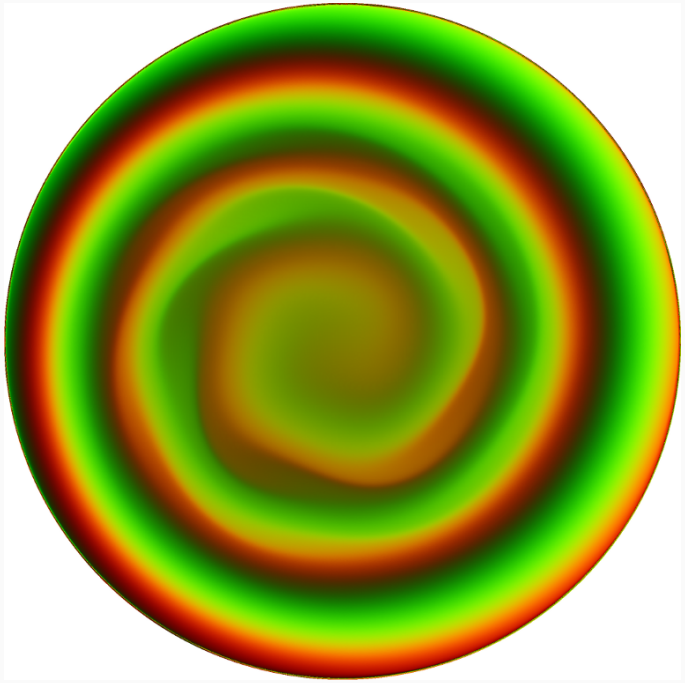

Figure 6: τ^{10}

Behavior of iterates

We discretize the first return map τ and then compute iterates. (here $\mu = 0.1$, $c = 2$).

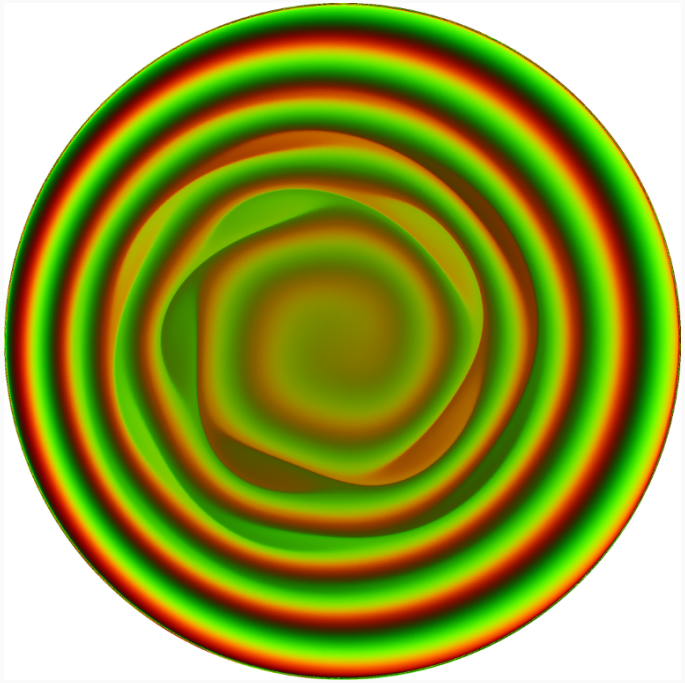

Figure 6: τ^{20}

Behavior of iterates

We discretize the first return map τ and then compute iterates. (here $\mu = 0.1$, $c = 2$).

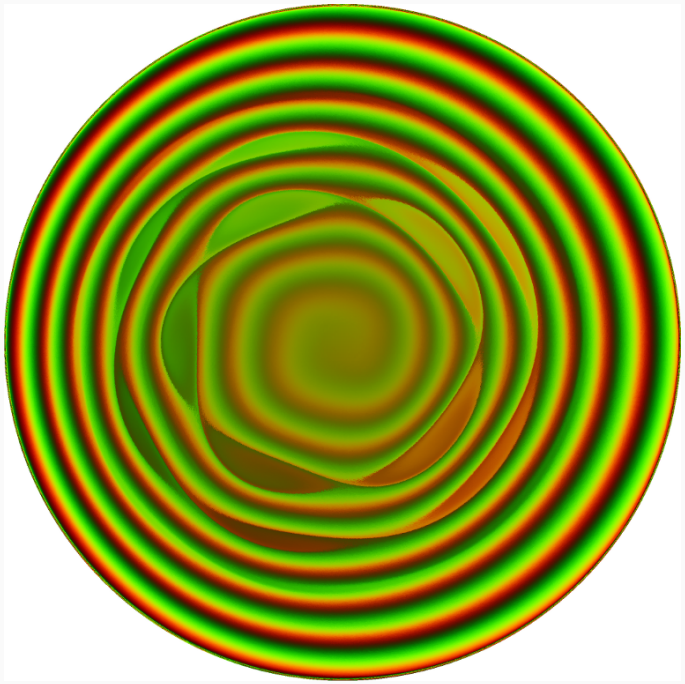

Figure 6:

The return map for the annulus

Twist and nontwist

- For small mass ratios or energies sufficiently far below L_1 the first return map is a twist map: the dynamics are relatively well-approximated by the rotating Kepler problem.
- (Nontwist?) map for larger μ, or c close to L_1.

We parametrize the annulus by $[0,1] \times [0,1]$. The yellow line is the image of $\{0\} \times [0,1]$.

$\mu = 0$ **(twist)**

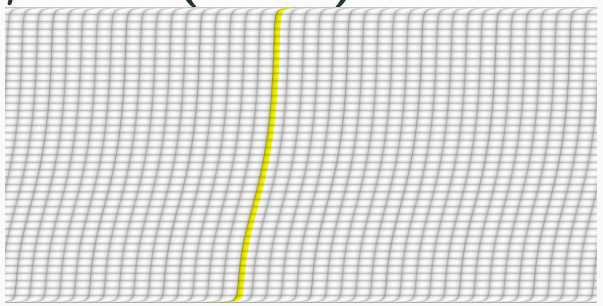

$\mu = 0.5325$

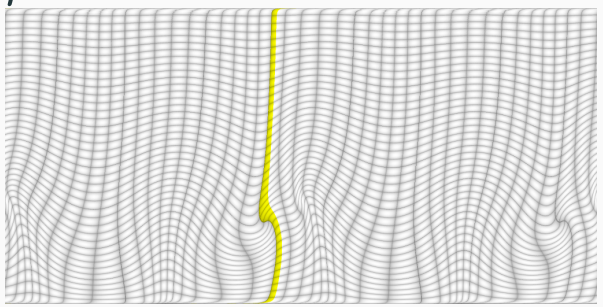

Return maps for Pluto near the critical energy

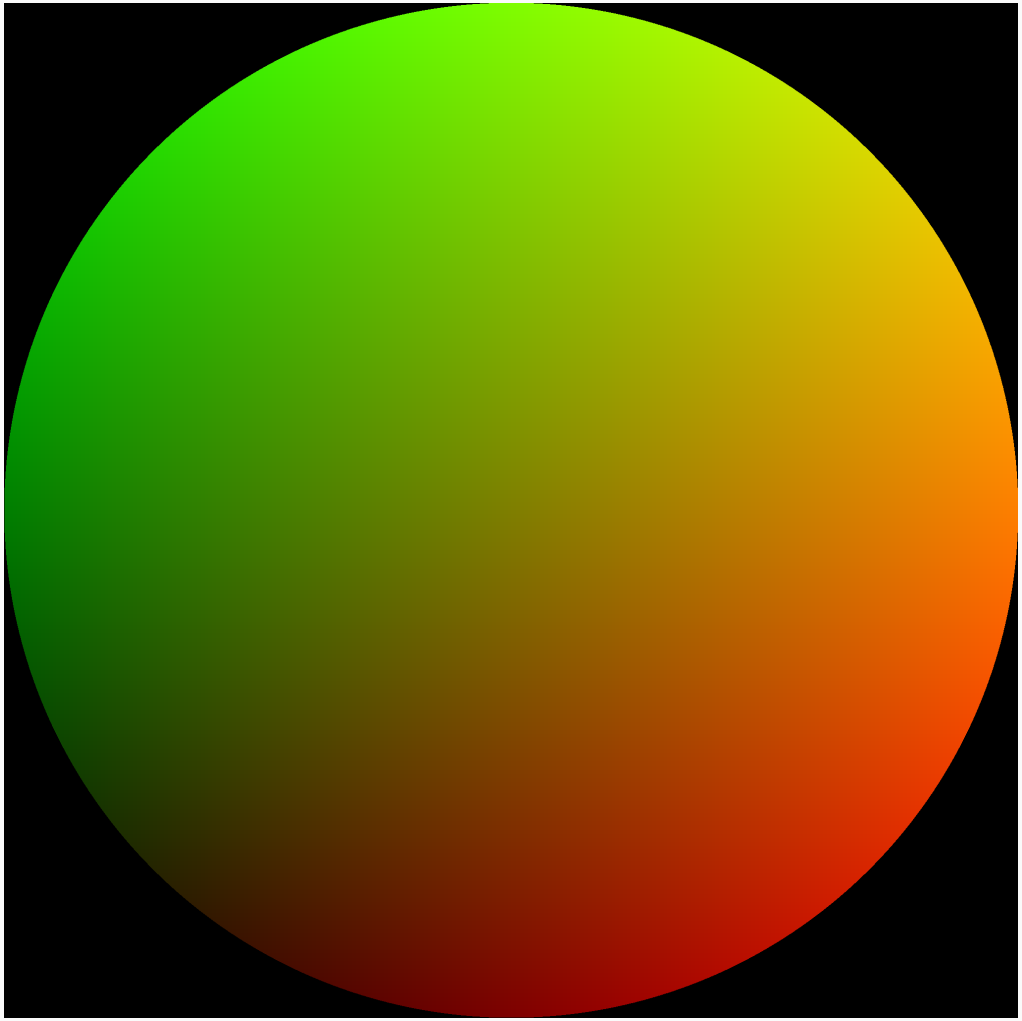

Return maps for Pluto near the critical energy

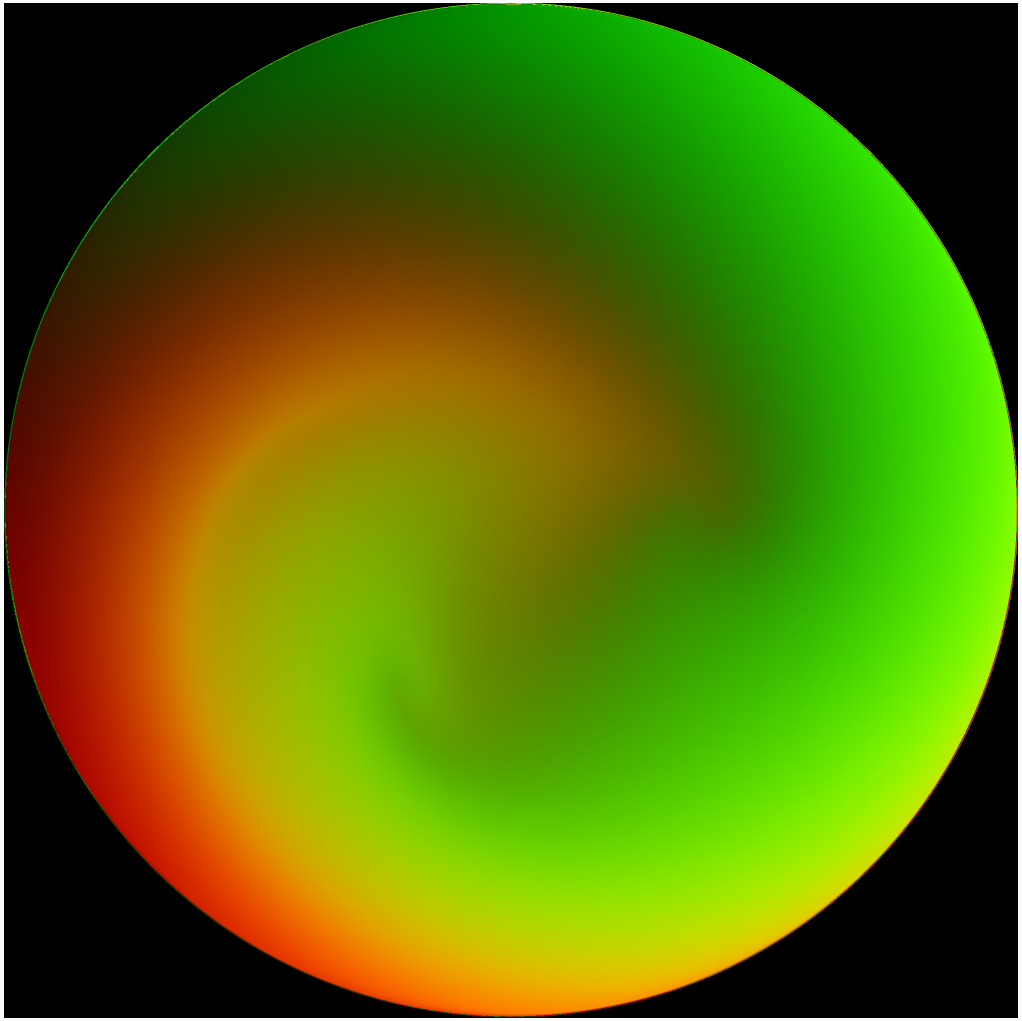

Return maps for Pluto near the critical energy

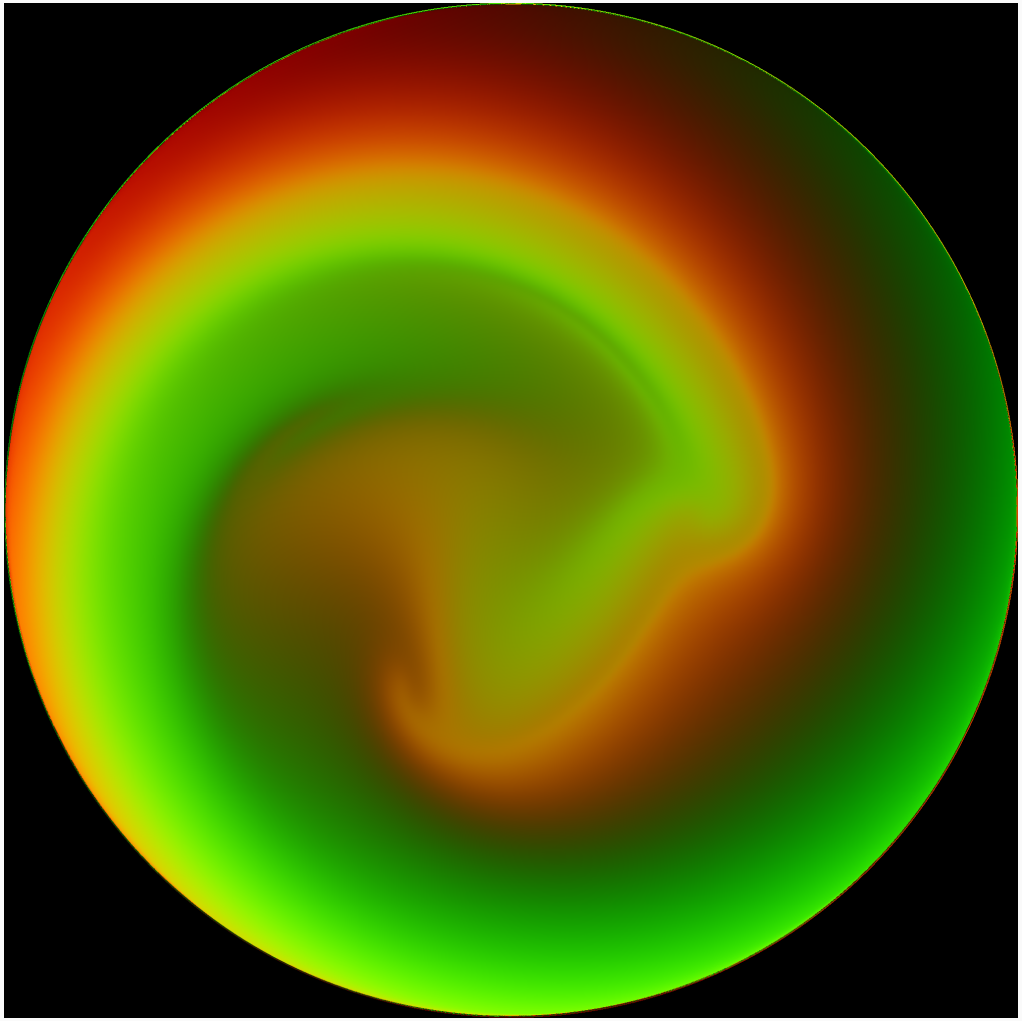

Return maps for Pluto near the critical energy

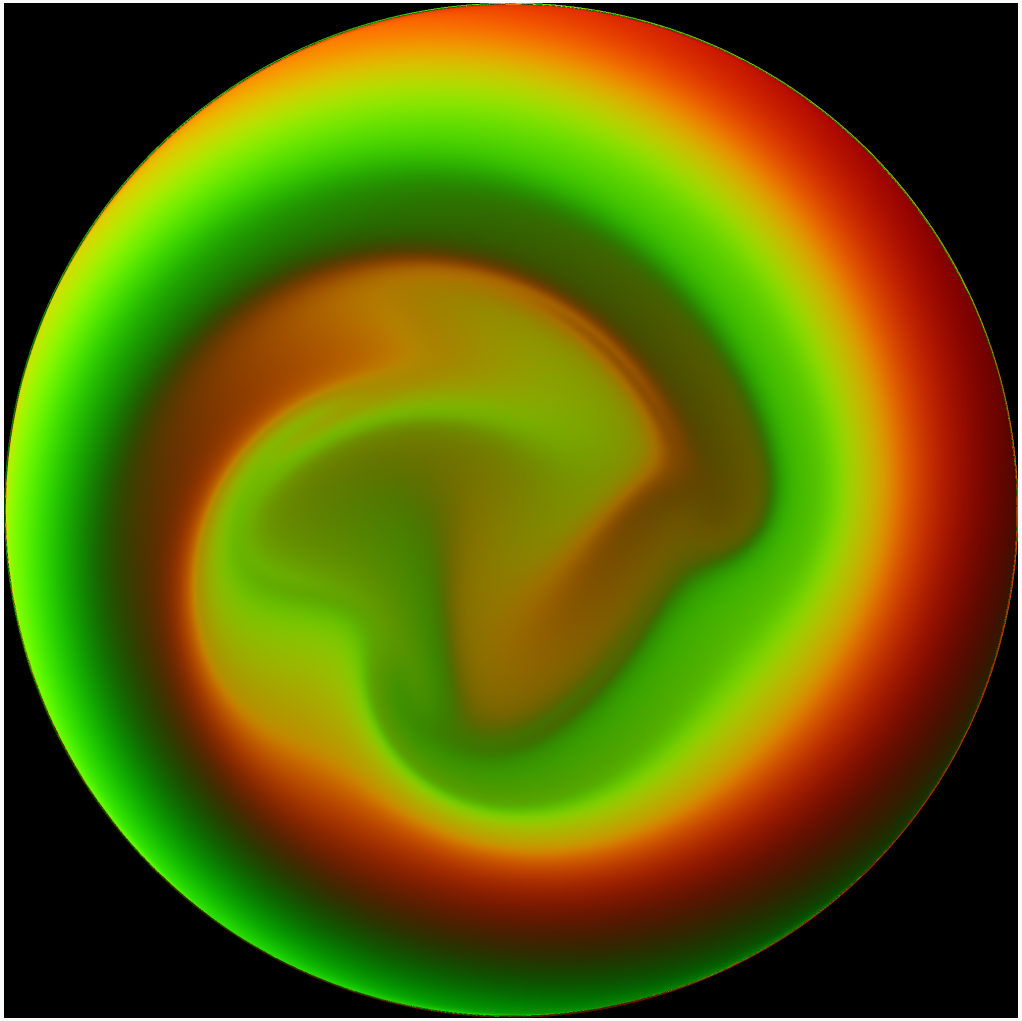

Return maps for Pluto near the critical energy

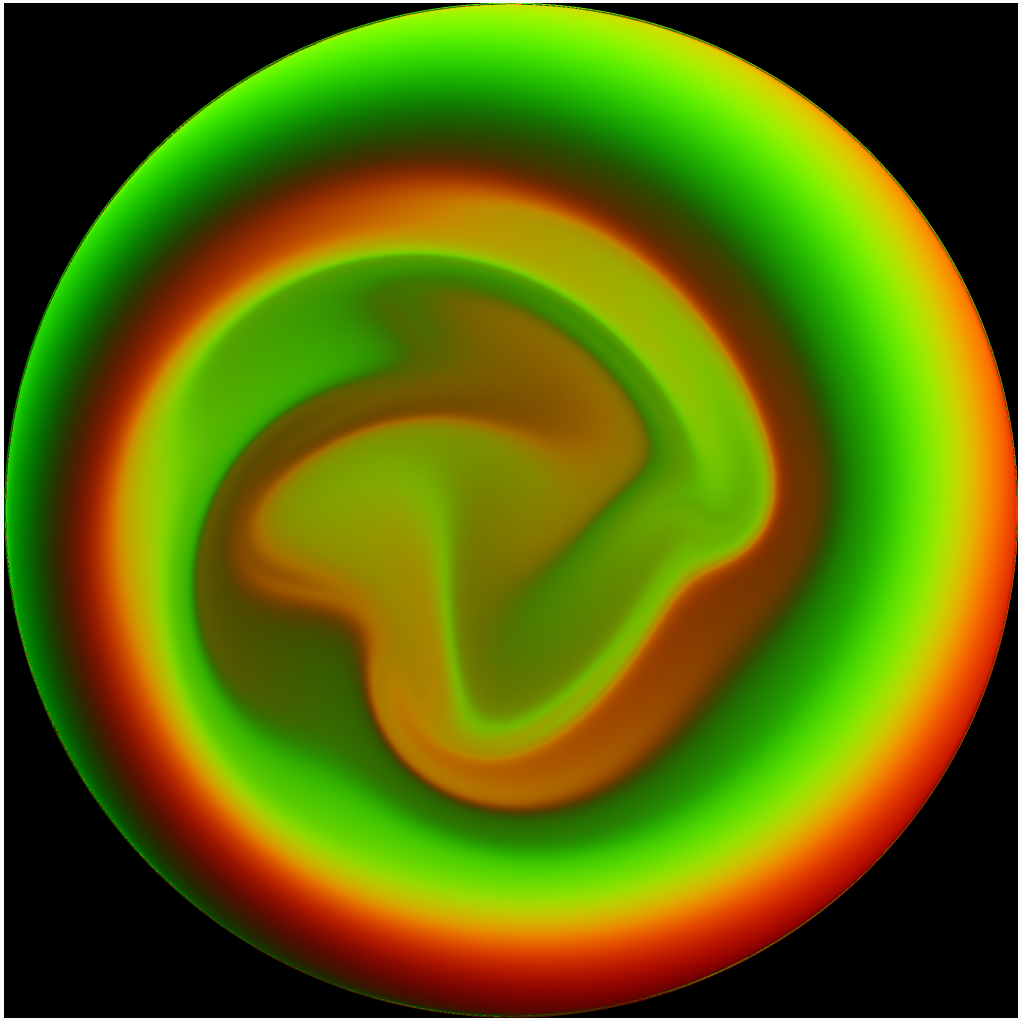

Return maps for Pluto near the critical energy

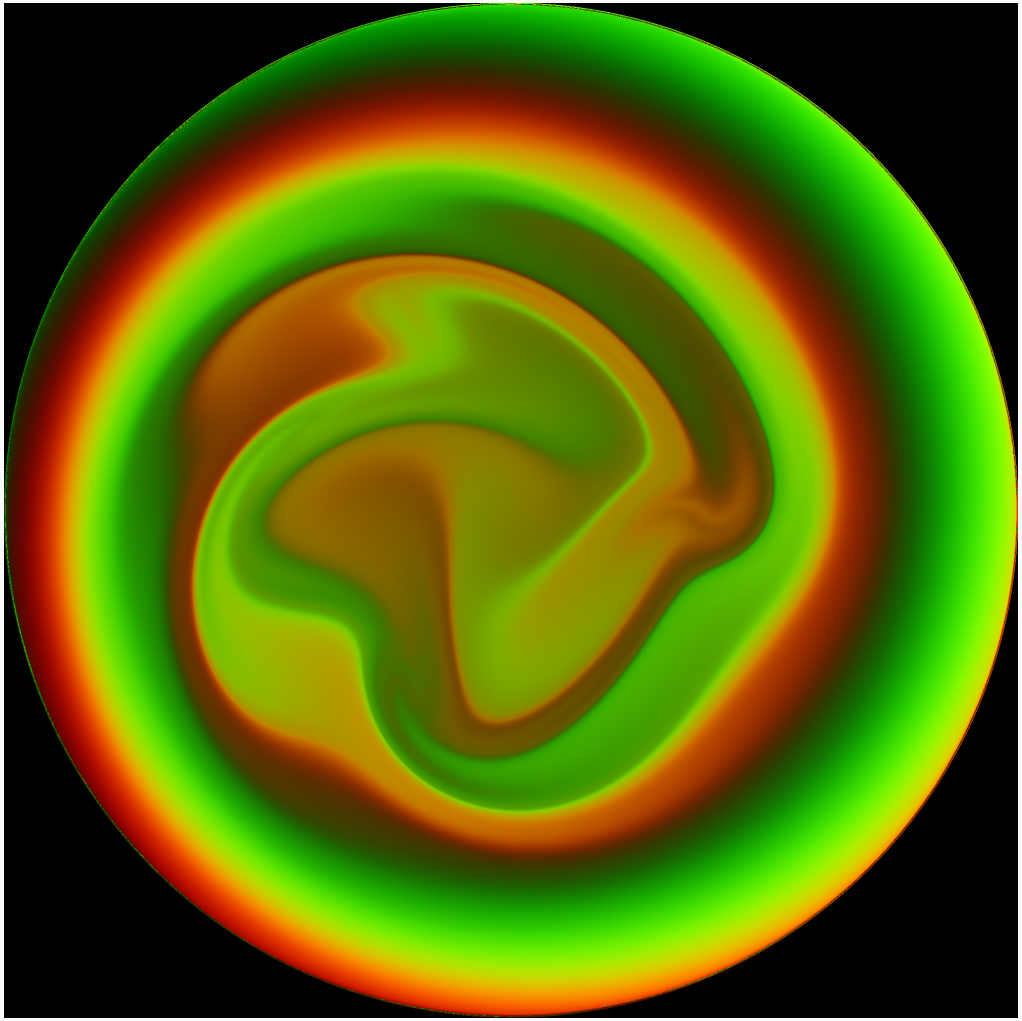

Return maps for Pluto near the critical energy

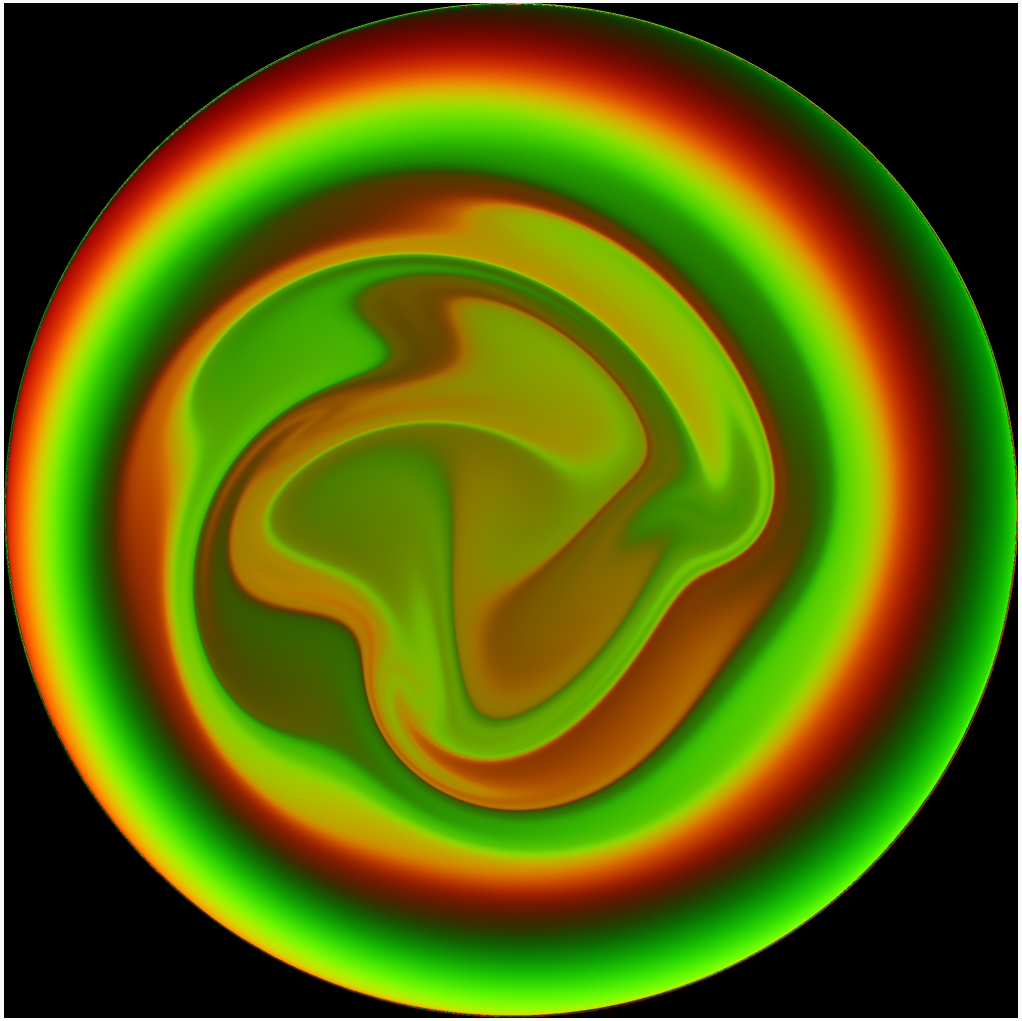

Return maps for Pluto near the critical energy

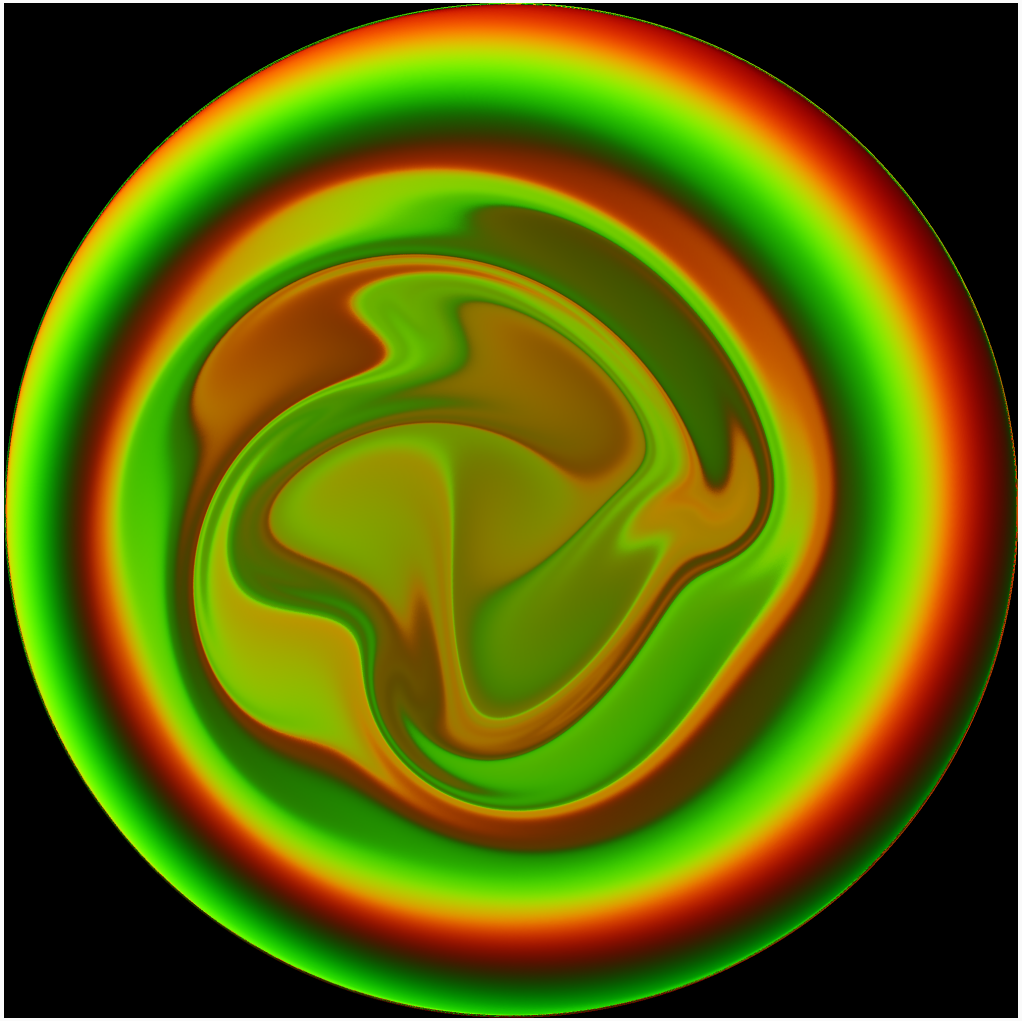

Return maps for Pluto near the critical energy

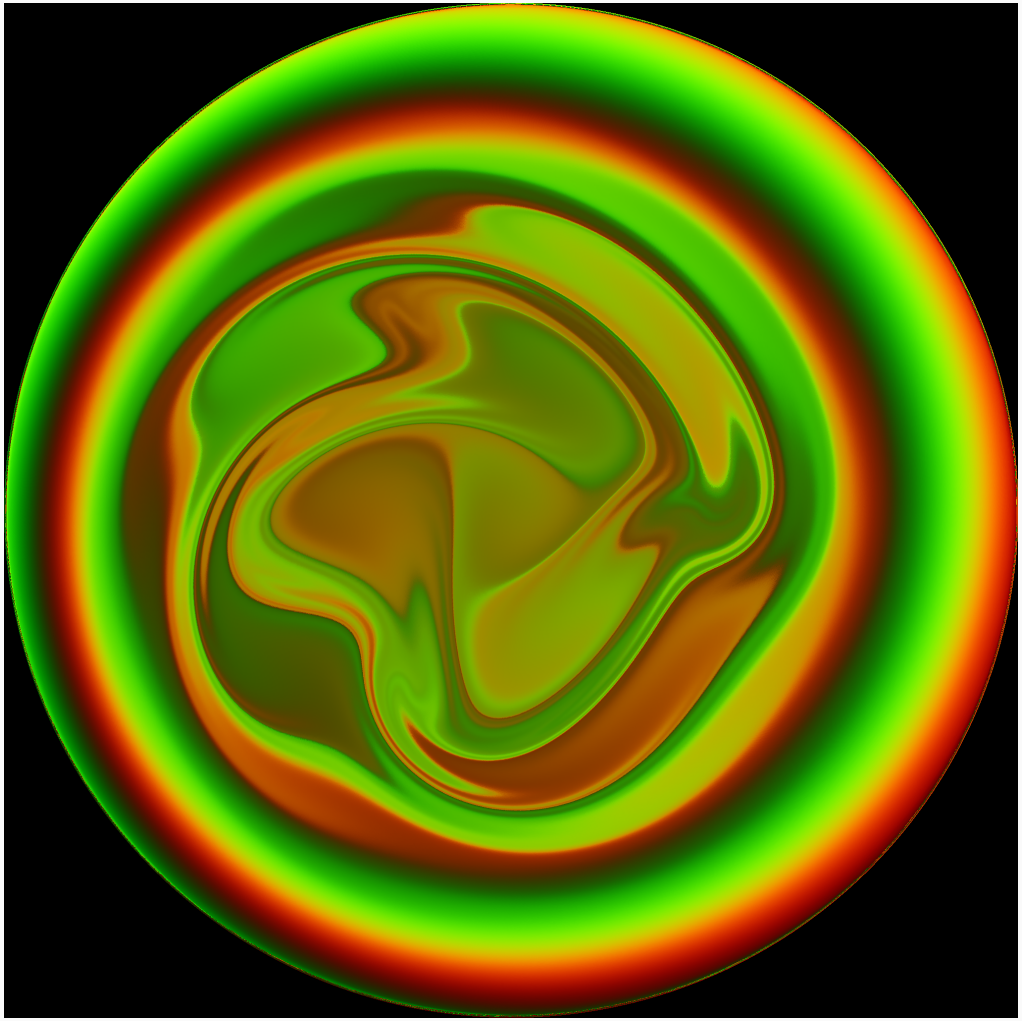

Return maps for Pluto near the critical energy

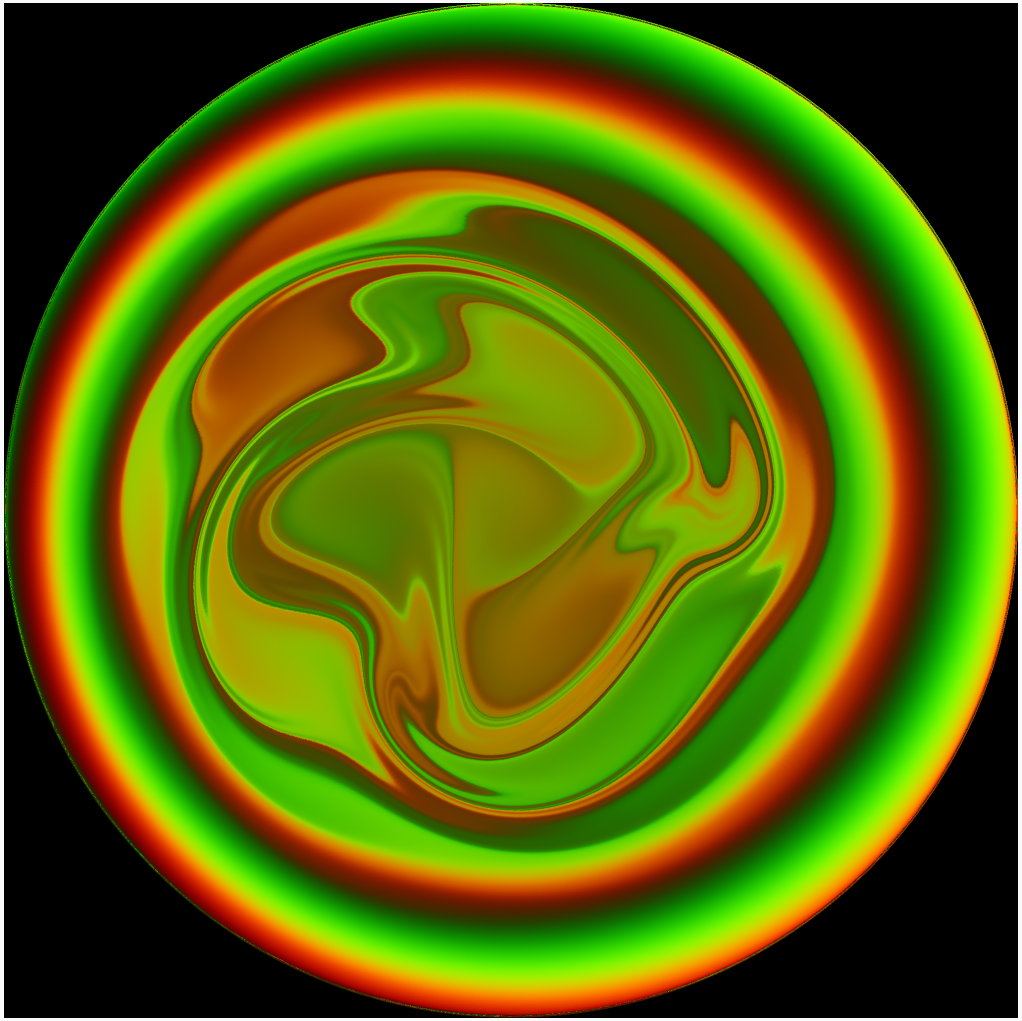

Return maps for Pluto near the critical energy

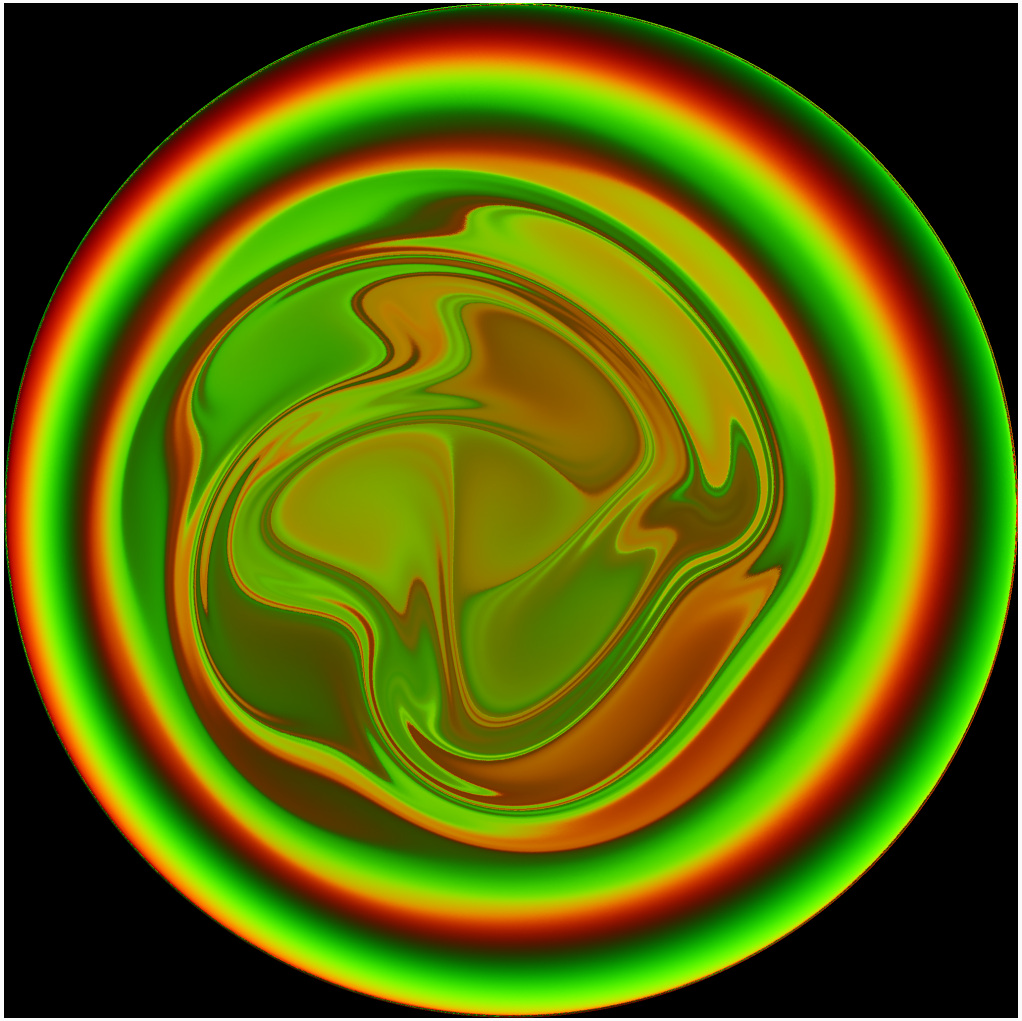

Return maps for Pluto near the critical energy

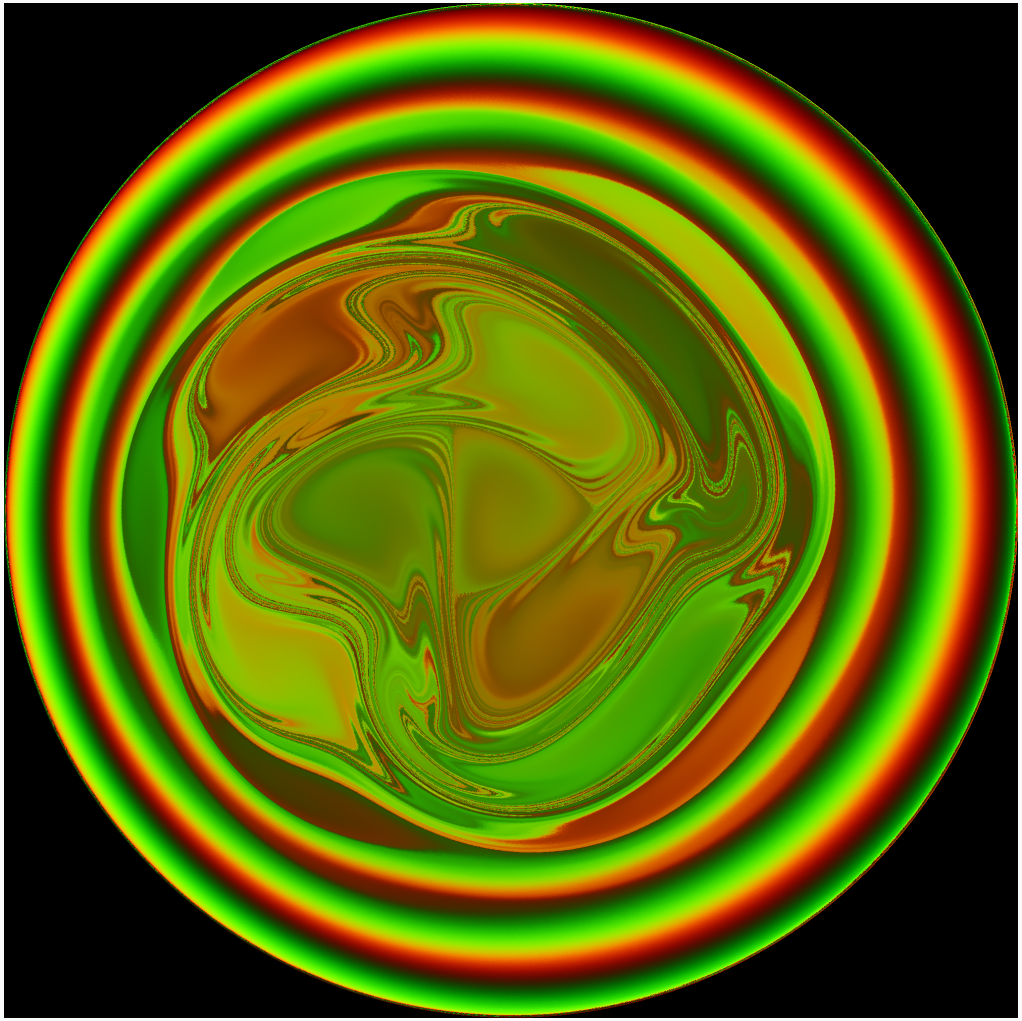

Return maps for Pluto near the critical energy

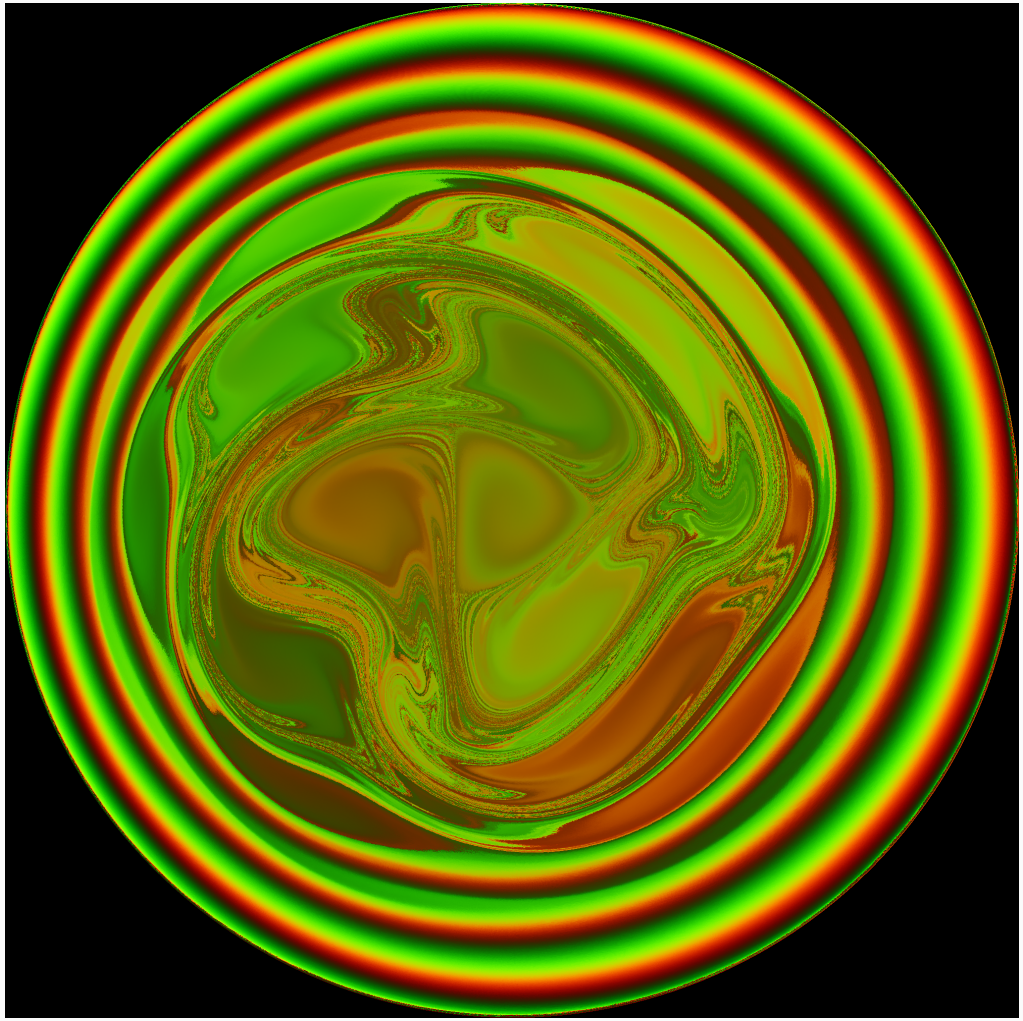

Return maps for Charon near the critical energy

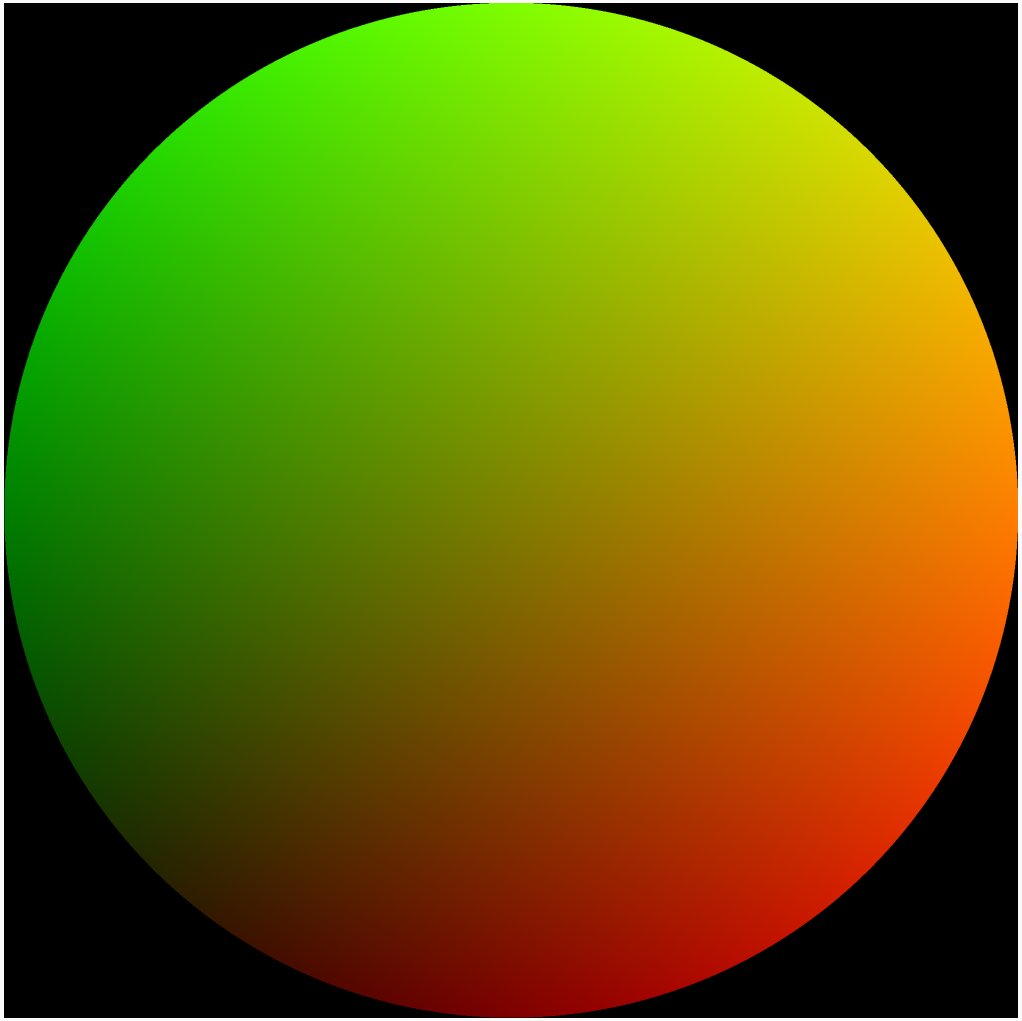

Return maps for Charon near the critical energy

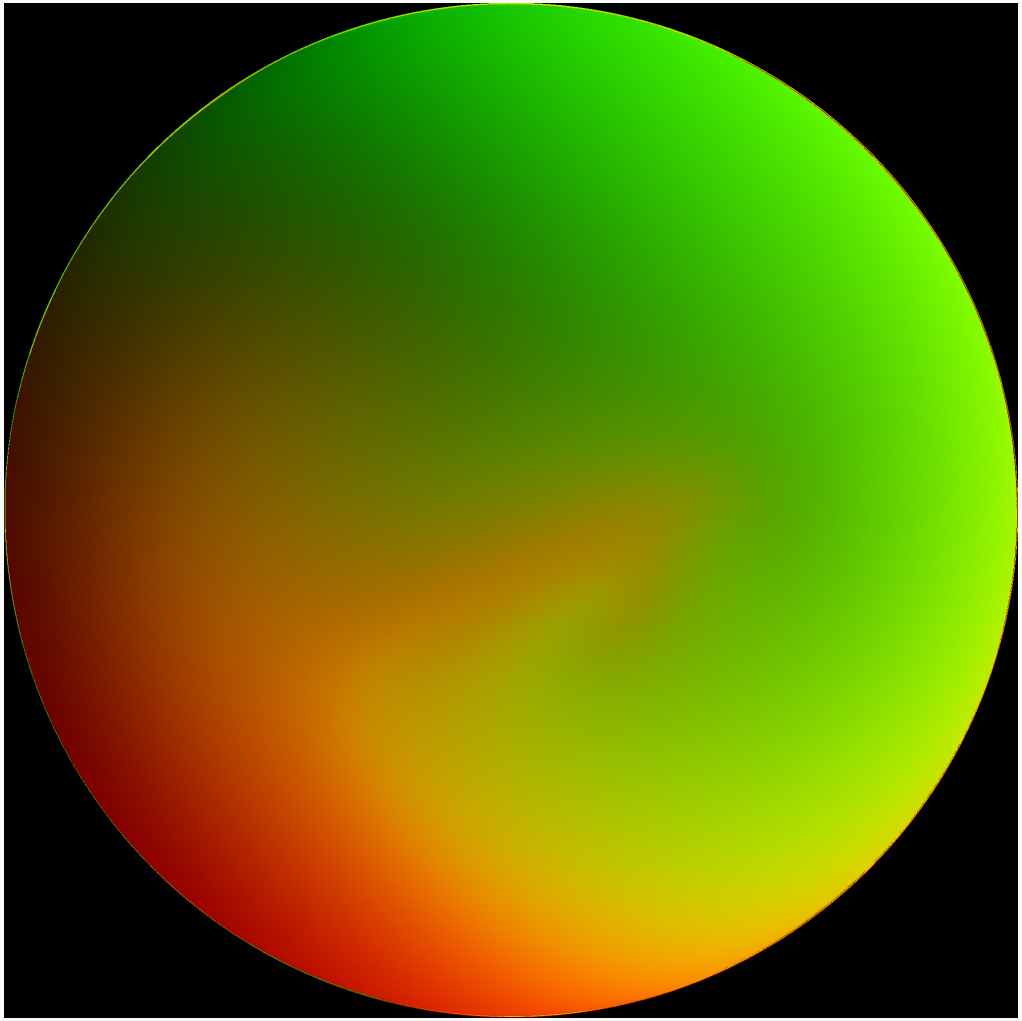

Return maps for Charon near the critical energy

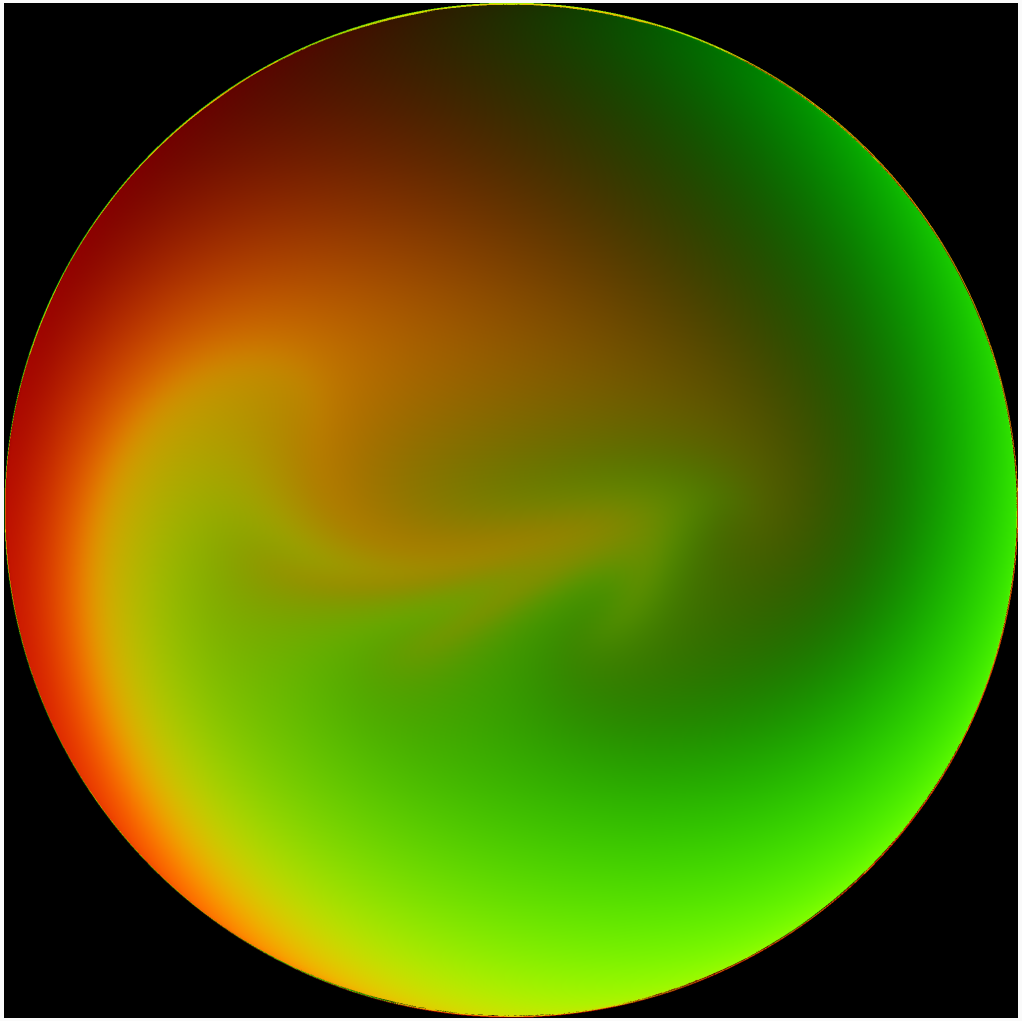

Return maps for Charon near the critical energy

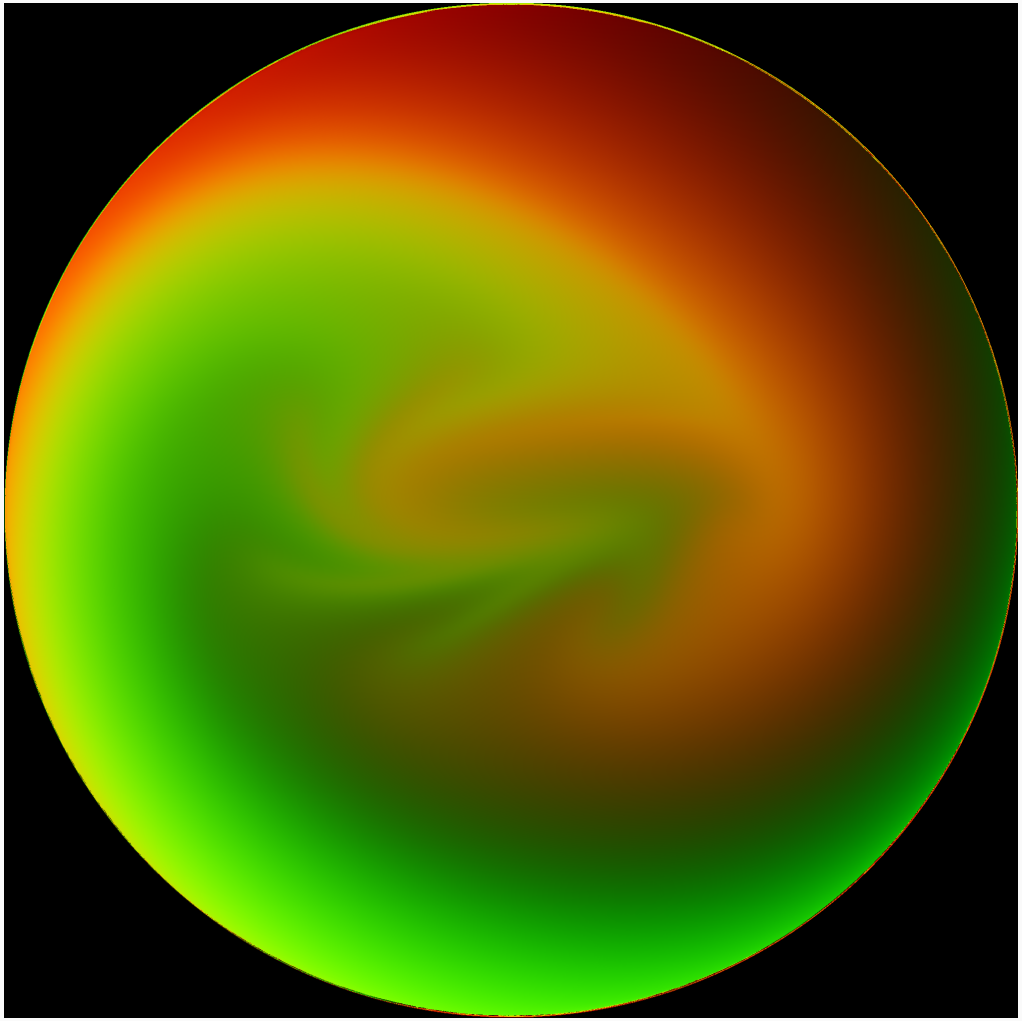

Return maps for Charon near the critical energy

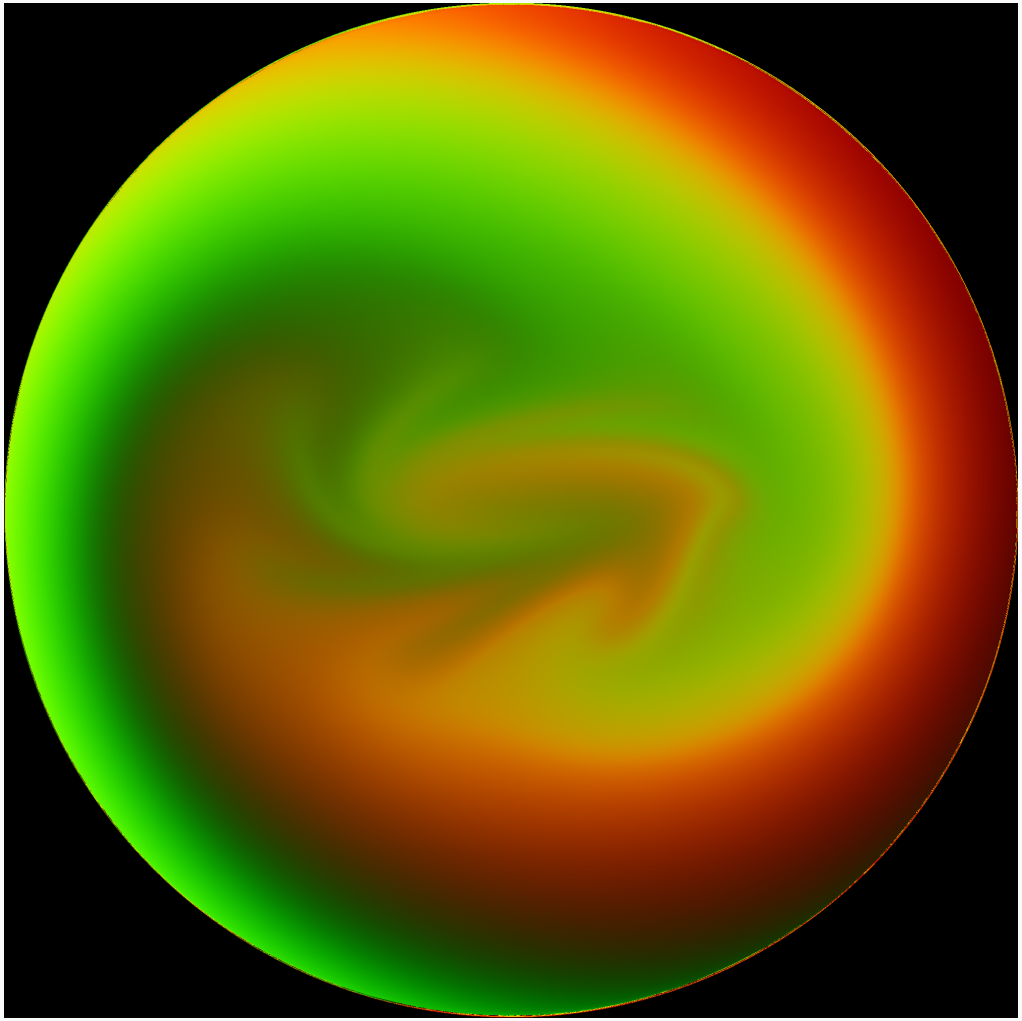

Return maps for Charon near the critical energy

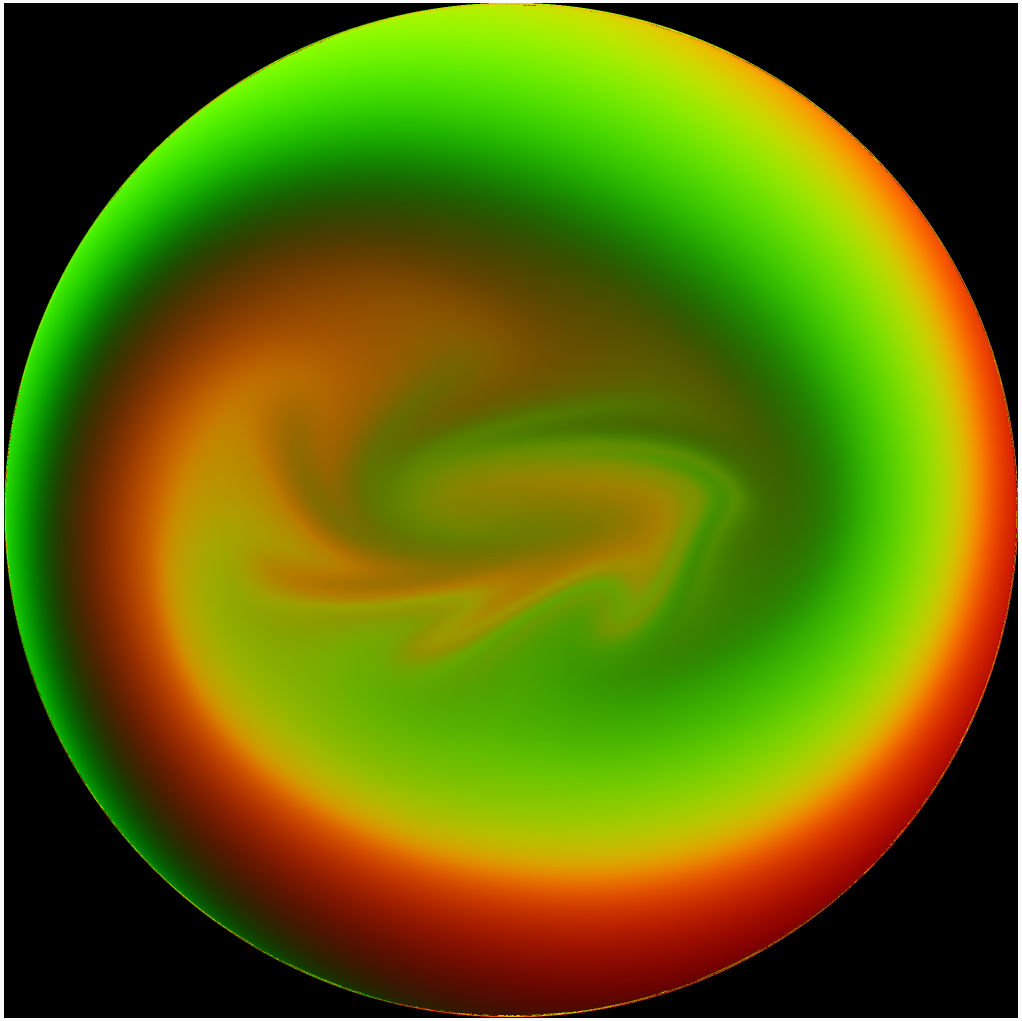

Return maps for Charon near the critical energy

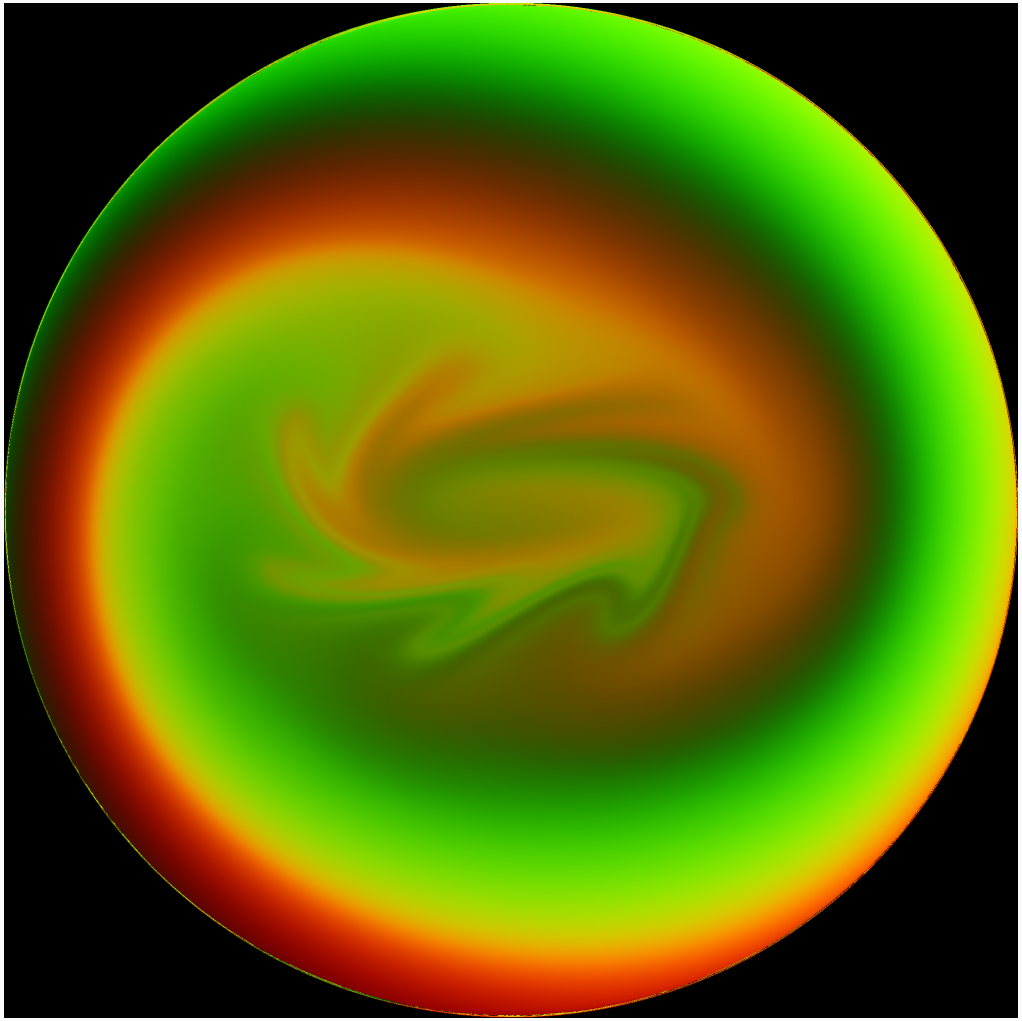

Return maps for Charon near the critical energy

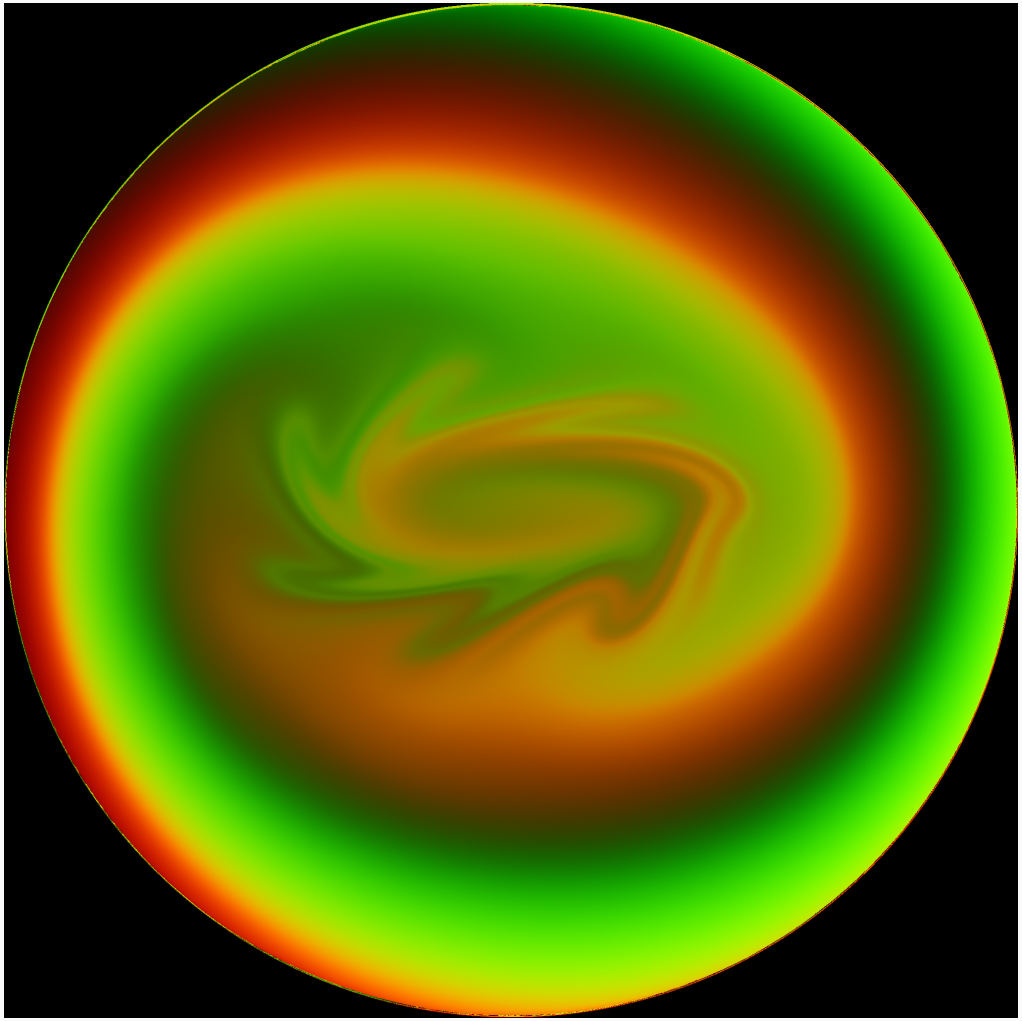

Return maps for Charon near the critical energy

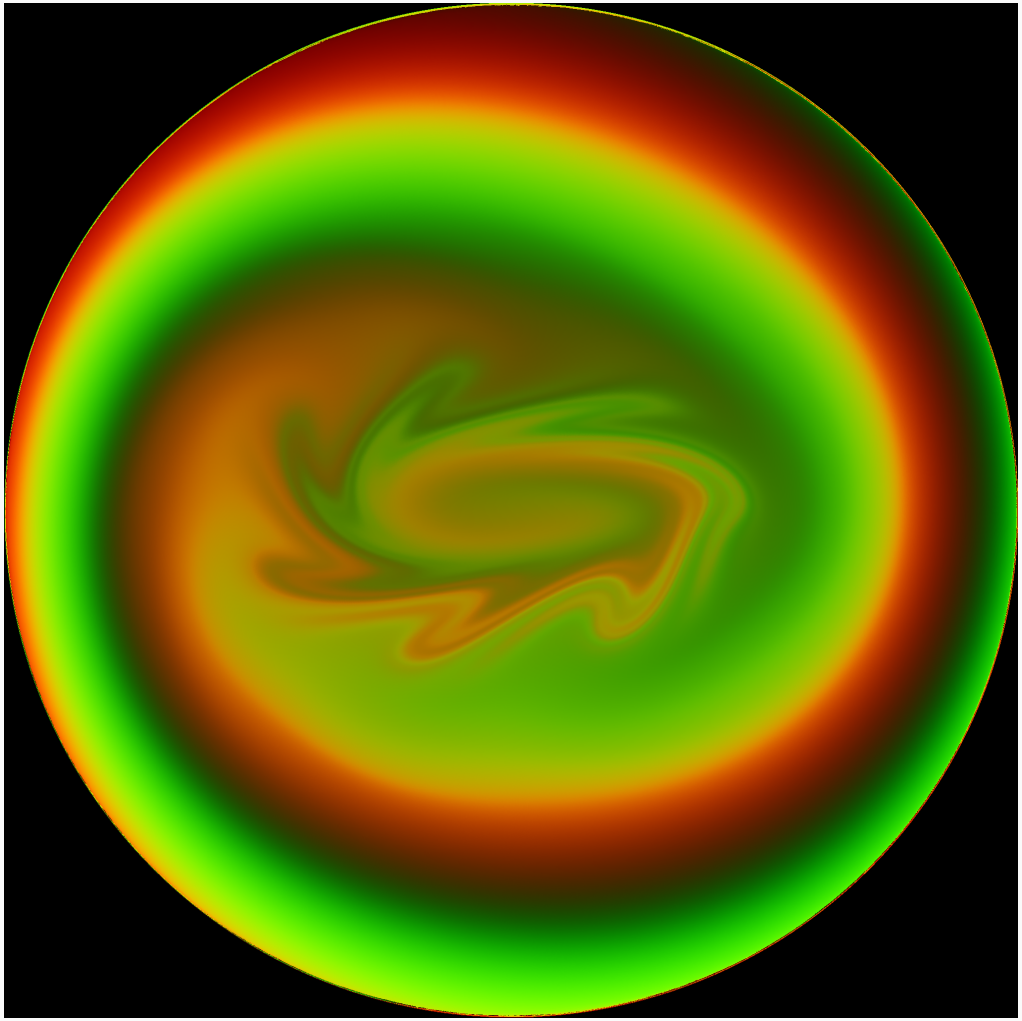

Return maps for Charon near the critical energy

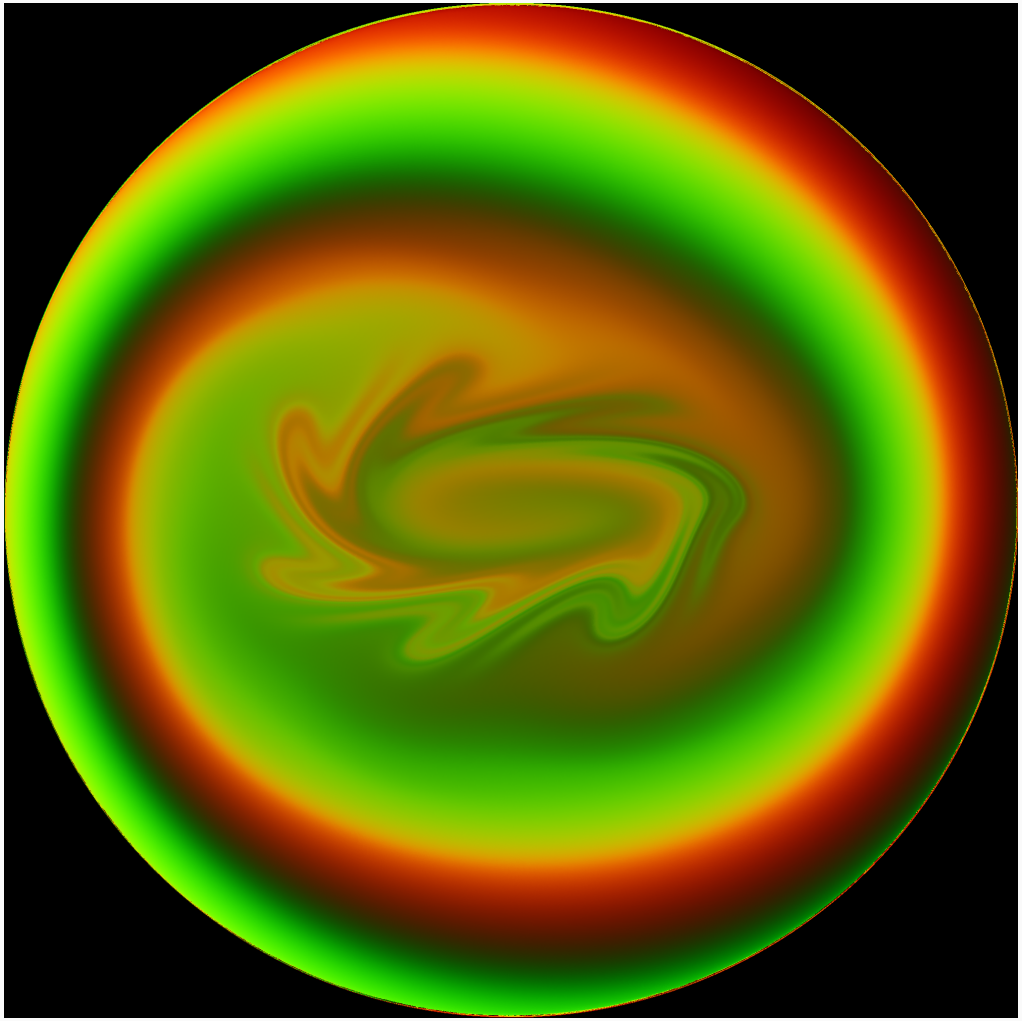

Return maps for Charon near the critical energy

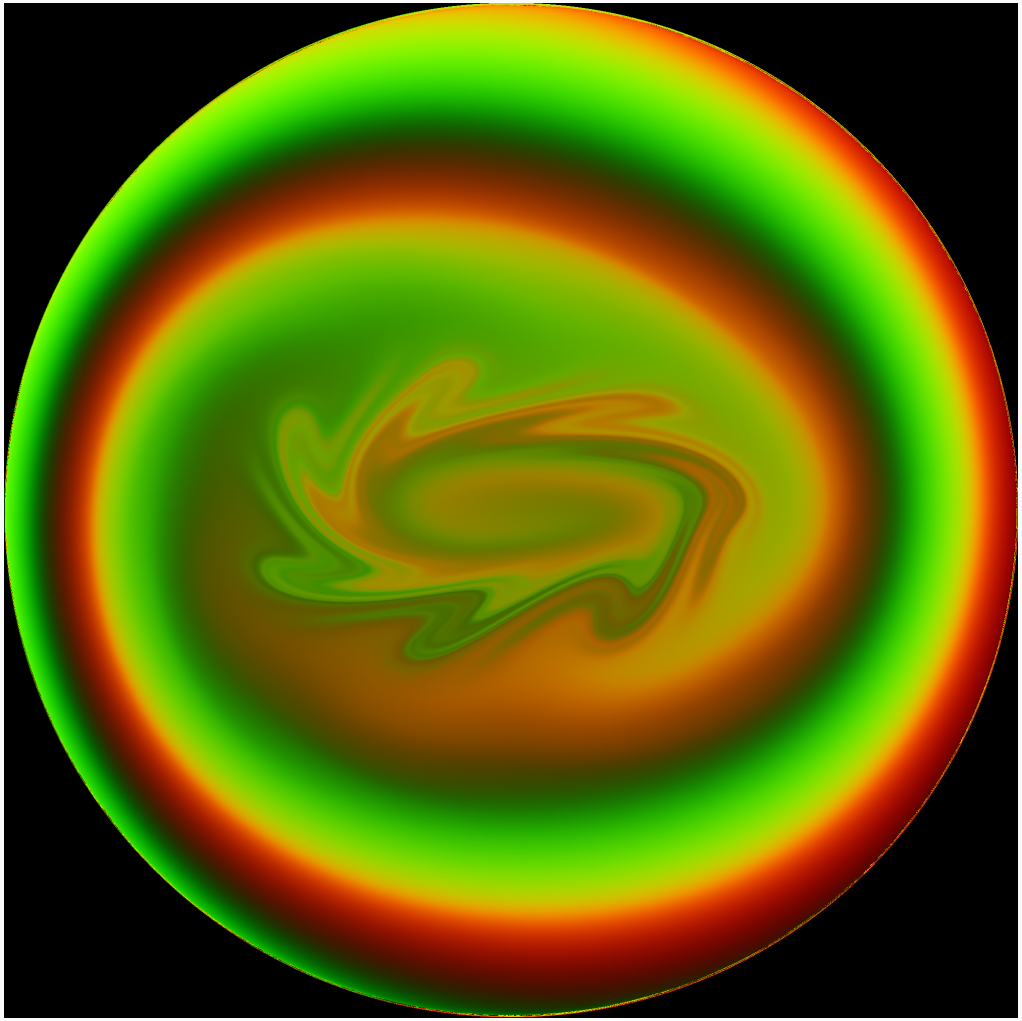

Return maps for Charon near the critical energy

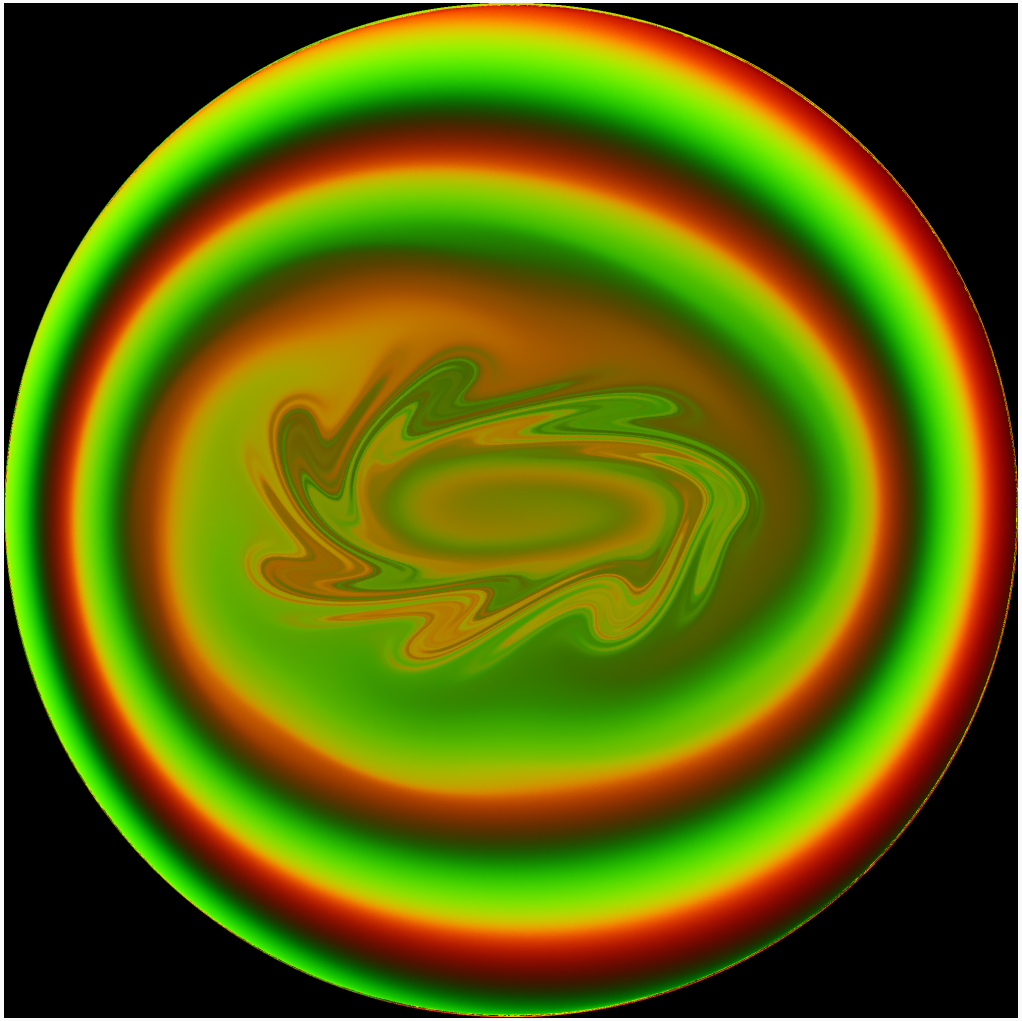

Return maps for Charon near the critical energy

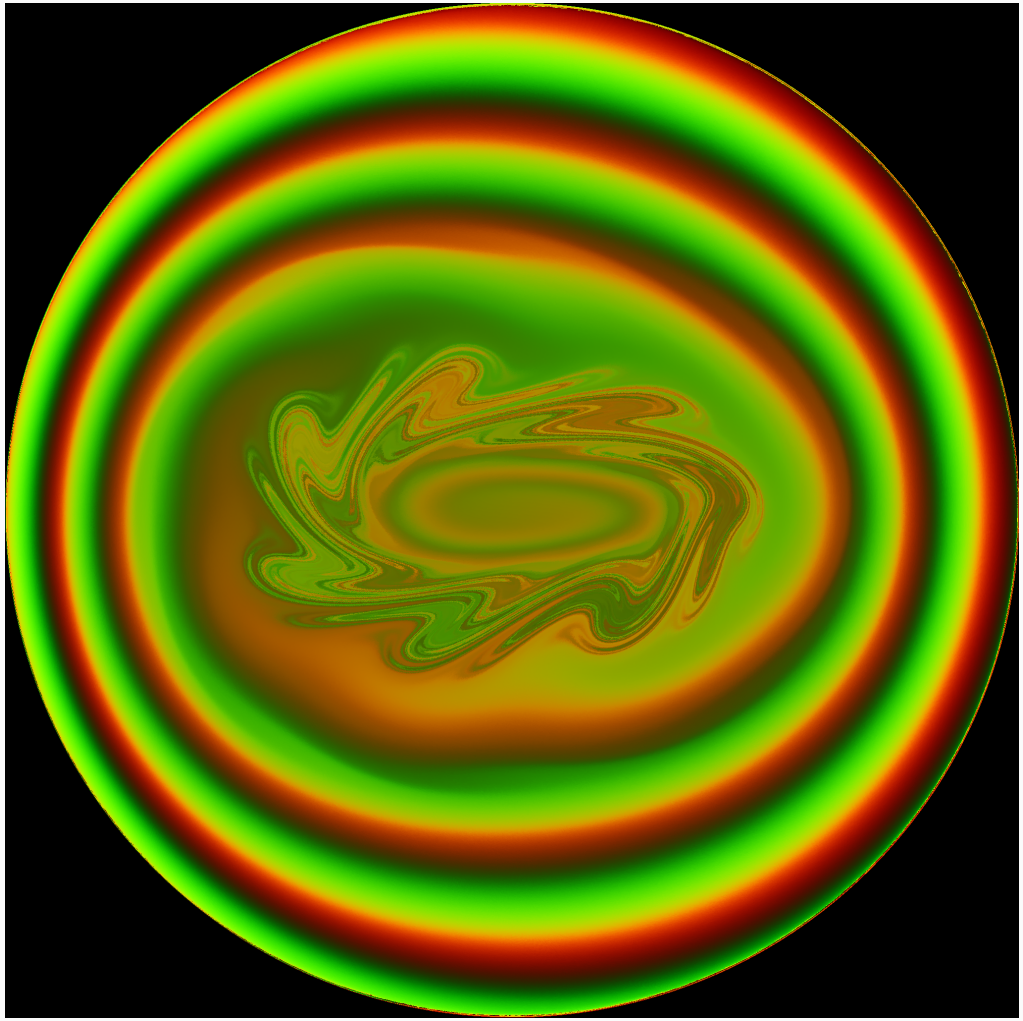

Collisional set

Consider the set of points on D that undergoes a collision at some point along its orbit, say $C_{\mu,c}$. For μ, $C_{0,c}$ is just a circle. If we approximate $C_{\mu,c}$ by looking at finitely manny iterations we find

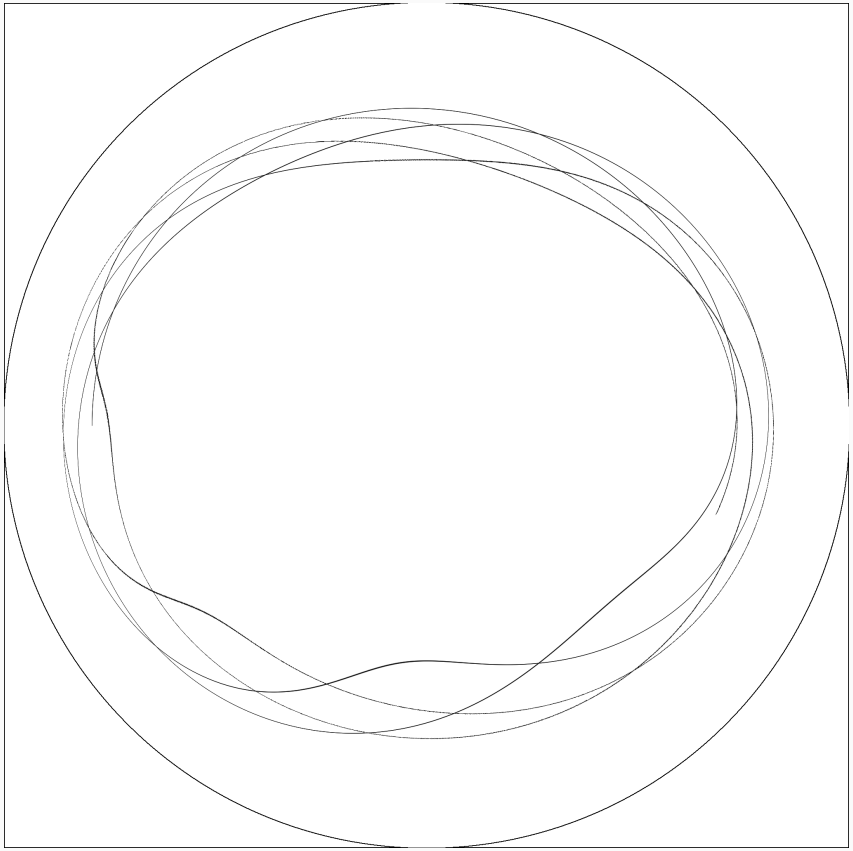

Collisional set

Consider the set of points on D that undergoes a collision at some point along its orbit, say $C_{\mu,c}$. For μ, $C_{0,c}$ is just a circle. If we approximate $C_{\mu,c}$ by looking at finitely manny iterations we find

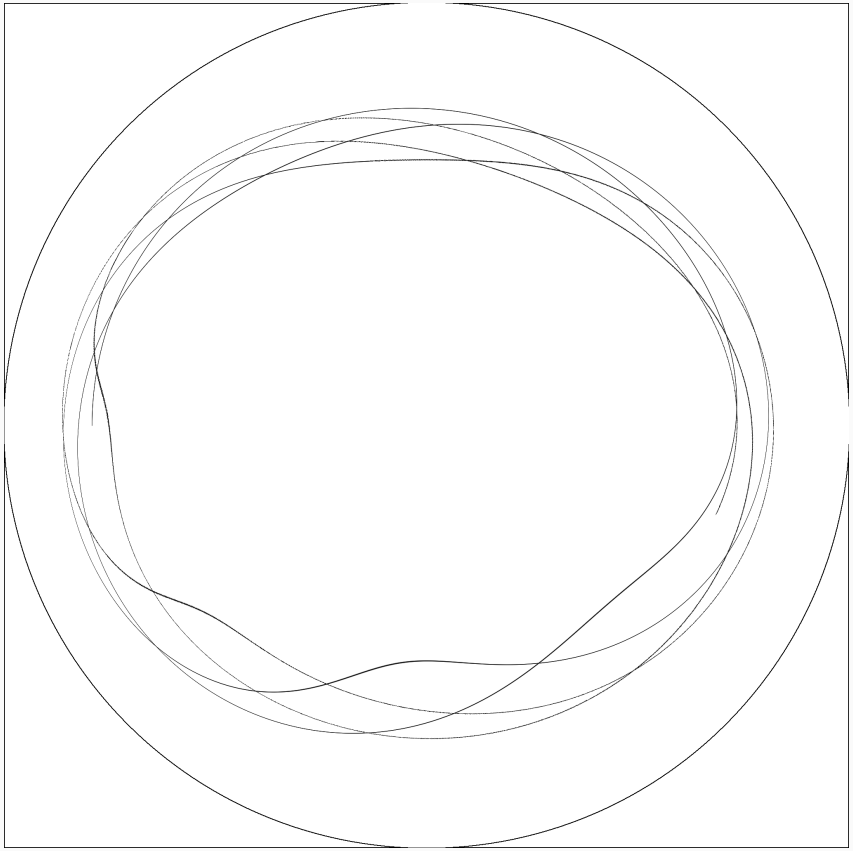

Collisional set

Consider the set of points on D that undergoes a collision at some point along its orbit, say $C_{\mu,c}$. For μ, $C_{0,c}$ is just a circle. If we approximate $C_{\mu,c}$ by looking at finitely manny iterations we find

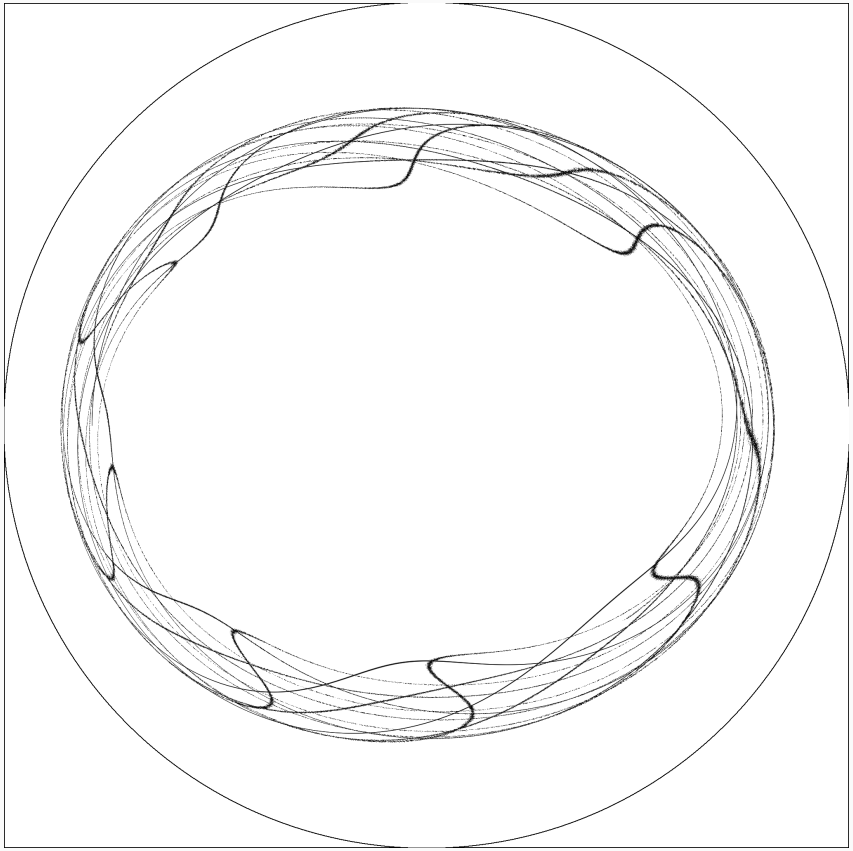

Collisional set

Consider the set of points on D that undergoes a collision at some point along its orbit, say $C_{\mu,c}$. For μ, $C_{0,c}$ is just a circle. If we approximate $C_{\mu,c}$ by looking at finitely manny iterations we find

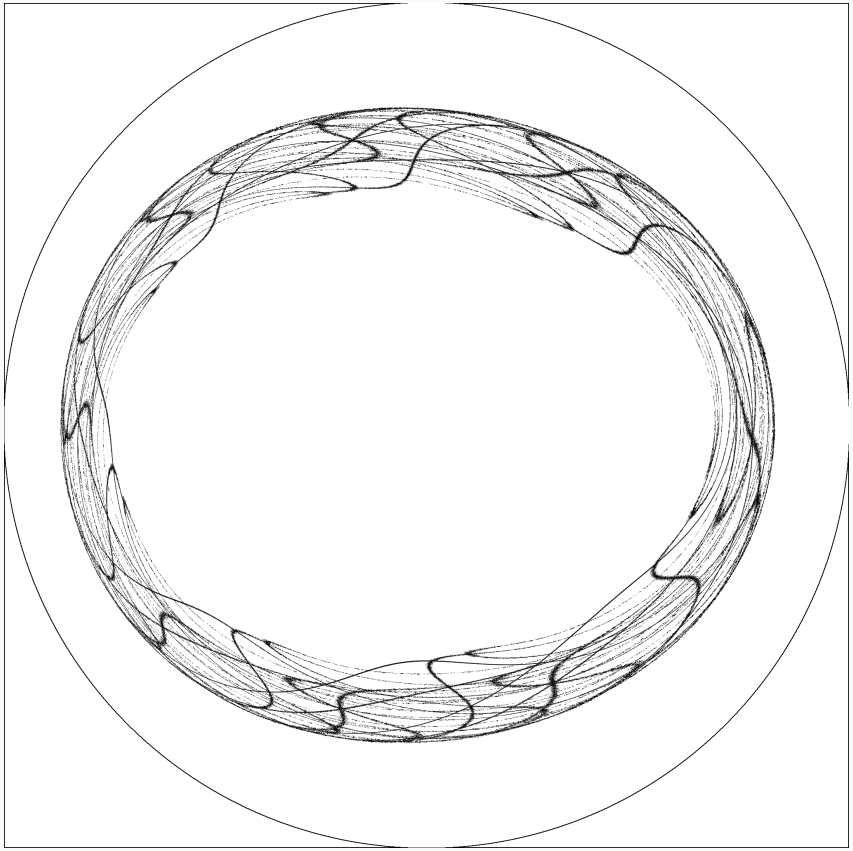

Collisional set

Consider the set of points on D that undergoes a collision at some point along its orbit, say $C_{\mu,c}$. For μ, $C_{0,c}$ is just a circle. If we approximate $C_{\mu,c}$ by looking at finitely manny iterations we find

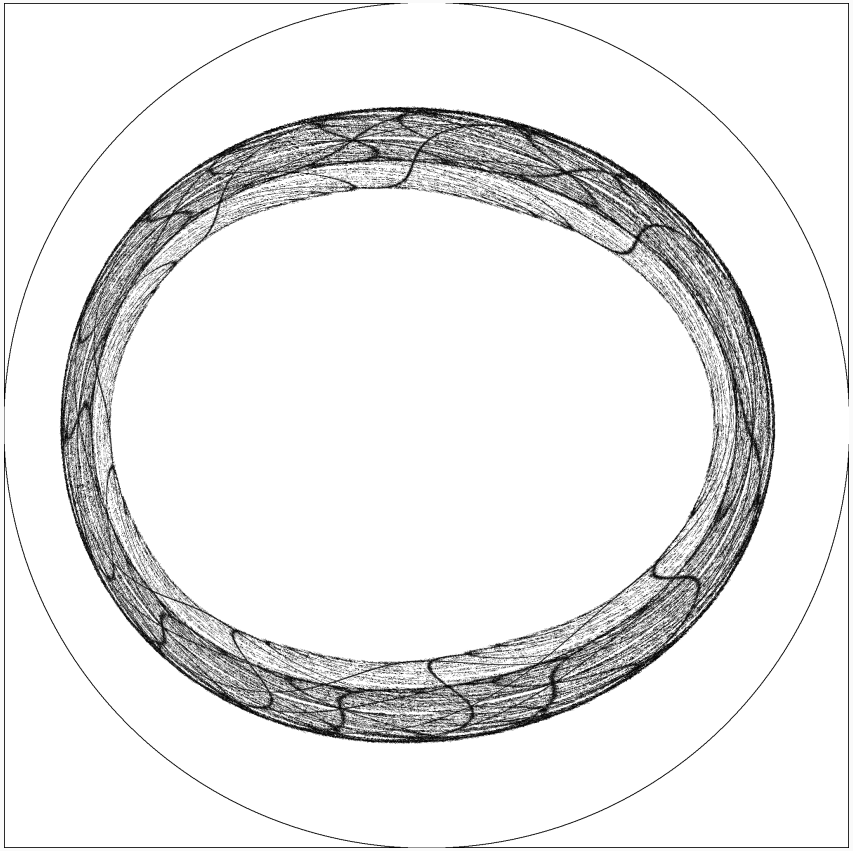

Collisional set

Consider the set of points on D that undergoes a collision at some point along its orbit, say $C_{\mu,c}$. For μ, $C_{0,c}$ is just a circle. If we approximate $C_{\mu,c}$ by looking at finitely manny iterations we find

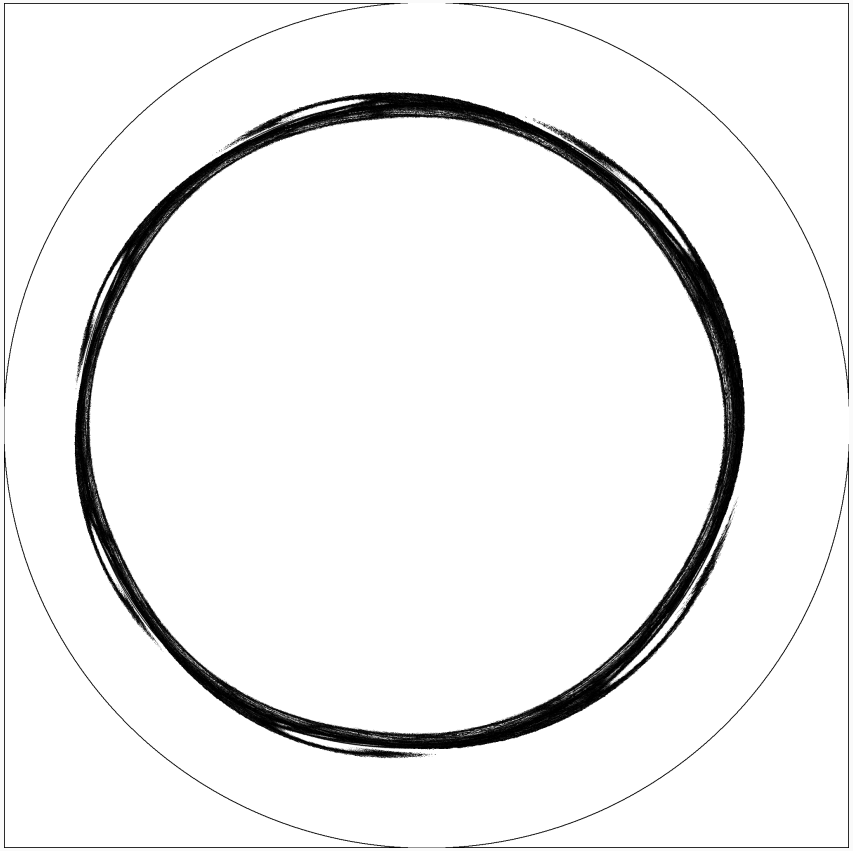

Thank you

謝謝